

Master's thesis

**Force and pressure feedback during  
epidural needle insertion in the  
ligamentum flavum of piglets**

**W.Boessenkool**

Delft, 9th of March 2012

Student Number: 1545019

Delft University of Technology  
Faculty of 3mE  
Department of BioMechanical Engineering



# **Force and pressure feedback during epidural needle insertion in the ligamentum flavum of piglets**

Wouter Boessenkool

Coaches:  
Dr. J.J. van den Dobbelsteen  
Ir. D.J. van Gerwen  
M. Vogt



## Preface

The master thesis what you are about to read is the result of a research on tissue feedback in order to improve the epidural anesthesia simulator, which is a product of the MISIT department of the Delft University of Technology.

First, the article written on the research is presented, followed by the background of the study. Appendix A deepens the anatomical background which is required to understand the research, where appendix B,C describe the experimental setup and the used protocol.

Appendix D shows an overview of the results. Appendix E describes the used statistical transformation and Appendix F shows some insight in the data analysis.

Finally, Appendix G shows some CT-images made during the experiments.

The content of this thesis covers an animal study which was performed in collaboration with an anesthetist and the anesthesia research department of Erasmus Medical Center.

Although research on living tissue is quite difficult and therefor the results vs. effort ratio was sometimes somewhat discouraging during the research, the results are quite interesting.

The results can help with improving patient safety.

I want to thank all people who contributed to this study. Special thanks to my supervisors, Dr. John J. van den Dobbelen and Ir. Dennis J. van Gerwen, for supporting and stimulating me in designing an experiment set-up and guide me all the way through. Also I would like to thank the clinical specialist, Dr. Mark Vogt, for his pleasant cooperation. Mark has provided his knowledge and expertise for this study which would not have taken place without him. At last I want to thank the MISIT department and my fellow students for providing a comfortable and friendly working environment.

Wouter Boessenkool



# Force and pressure feedback during epidural needle insertion in the ligamentum flavum of piglets.

Wouter Boessenkool<sup>1</sup>, John van den Dobbelen<sup>1</sup>, Dennis van Gerwen<sup>1</sup>, Mark Vogt<sup>2</sup> and Jenny Dankelman<sup>1</sup>

**Abstract**—Epidural anesthesia is a commonly used anesthesia method during surgery or giving birth to a child. During the insertion of the needle in the back of the patient, the anesthetist has to interpret the different forces which requires extensive skills. To obtain these skills the residents train on patients, which is not without risk. Due to a lot of variation in anatomy of the human body, the identification of the tissues can be very difficult. An epidural anesthesia simulator can reduce this risk by offering anesthetists the opportunity to experience the differences in force and pressure feedback of the different tissues before moving on to patients. In literature only very little is available about needle-tissue interaction around the epidural space. To collect data about tissue resistance during the insertion of an epidural needle, tests were done on living piglets. These animal tests were done at Erasmus MC, Rotterdam. During needle insertion, the position of the needle was captured along with the force on the needle and the pressure in the needle. Pressure measurements were used for the epidural space identification. The most important force feedback during the insertion is a force-peak which occurs by puncturing the ligamentum flavum. At the moment the needle tip enters the epidural space, a pressure-drop in the needle occurs which is the most important pressure feedback.

The measured force-peak with a 18G epidural needle can be described by a lognormal distribution and lies in the 68.3% confidence interval of 5.45 till 11.03 N and has a geometric mean of 7.754 N. The distance between the force-peak event and the pressure-drop event can be described with a normal distribution with a mean of 1.17 mm ( $s=1.217$ ), where a positive value means that the force event occurs before the pressure-drop. The experimental results showed that there is no systematic difference in force peaks between piglets and neither between vertebrae. The measured pressure data showed that the pressure gradient is time-dependent when using a constant flow of liquid. Since it is unknown if an eventually 'tissue absorption' ratio of the ligamentum flavum is velocity dependent, no valid statements can be done based on this data. Another observation was that the force-peaks measured in deceased tissue (1-5h) are in the same range as the force-peaks in living tissue.

**Index Terms**—Epidural, medical simulation, force feedback

## 1 INTRODUCTION

In the development of the modern civilization, the discovery of anesthesia has been an important milestone. During the ages gradual improvements were made and in 1933 prof. A.M. Dogliotti [2] published for the first time about 'peridural anesthesia', nowadays known as epidural anesthesia. With this method a local anesthetic block can be applied, which has great benefits above total anesthesia. The greatest impact epidural anesthesia had was in obstetric anesthesia. In this application the procedure is performed at the lumbar region of the vertebral column. The procedure requires extensive skills of interpreting the resistance forces of different tissue. Research indicates that for an insertion successrate of 80%, around 90 procedures are needed [4]. Clinicians obtain their first experience on patients at lumbar level, where the risk of medical complications is the lowest.

### 1.1 Anatomy

The spinal cord of the human body consists of nerves coming from and going to the brain. They can roughly be separated in motor nerves for actuating the muscles and organs and sensory nerves for feedback. When blocking the nerves which conduct information leading to the perception of feeling, the brain does not detect that something is wrong. For example, this technique is used during surgery and obstetrics. The spinal cord is protected by the meninges (respectively dura mater and arachnoid) and the space around (epi) the dura mater is called the epidural space, see figure 1. When injecting analgesia in the epidural space, only the spurs from the spinal cord are blocked, which has as result that the nerves going to body parts below the place of injection are still functional. In order to get to the epidural space,

the needle has to penetrate skin, muscles and ligaments, see figure 1. To perform this insertion the anesthetist has to rely on tactile feedback to discriminate between the different tissues. This demands an extensive skill of interpreting the forces due to resistance of the tissues. In extreme cases such as obese patients or patients with shrunken spines due to osteoporosis, it is very difficult to perform.

The most obvious structure, the ligamentum flavum, can be identified by the rubbery structure of the tissue. After entering the epidural space the needle has to be stopped to avoid overshoot, which can result in puncturing the meninges (dural tap) and nerve damage in the spinal cord, where the risk depends on the place at the vertebral column. However the chance on leakage of cerebrospinal fluid (CSF) after dural tap, with headache as a result, is the same at all regions.

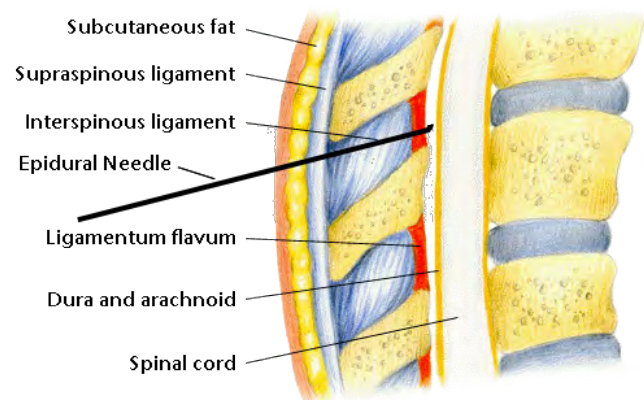


Fig. 1. Intersection of vertebral column, with the needle tip in the epidural.

<sup>1</sup> Department of BioMechanical Engineering, Faculty of 3mE, Delft University of Technology, Mekelweg 2, Delft, The Netherlands, (contact: j.j.vandendobbelen@tudelft.nl)

<sup>2</sup> Erasmus MC-Sophia, Dr. Molewaterplein 60, 3015 GJ Rotterdam, The Netherlands, (contact: m.vogt@erasmusmc.nl)

## 1.2 Simulator

In order to obviate the risk of medical complications the use of simulators is investigated by multiple parties. Simulators cannot completely replace training on patients, but it can be an addition in the current training programme in order to extend the skills of the resident before moving on to patients. The MISIT department of the TU-Delft is developing a 2DOF epidural simulator which can simulate force as a function of the position of the needle. With actual force data this can give an accurate simulation of the ligaments in the vertebral column. At this moment the simulation is loosely based on the very limited force-position data found in literature. Brett et al. [1] published a research where Tuohy needles were inserted into deceased porcine ligamentum flavum (decay-time of 2-5 hrs) using automated insertion. The size of the needle and the sample size of this research are unknown. Although somewhat unclear, it appears that the peak force measured in the ligamentum flavum is around 15 Newton. However, automated insertion obviates important tissue feedback. Therefore it is possible that the measurements include contact with unattended tissue, such as bone, causing an error in the found tissue characteristics. Furthermore it is not yet possible to simulate the pressure-drop inside the needle at the moment the needle tip enters the epidural space, which is an important part of the feedback in the epidural anesthesia procedure. Besides the force-position data, the pressure-position data in reality are unknown. The variance between vertebral ligaments in patients and the variance between patients is totally virgin territory.

## 1.3 Procedure of epidural anesthesia

Before the procedure the anesthetist determines between which vertebral disks and in what angle the needle has to be inserted. The angle of insertion depends on the position of the vertebrae, which can be quite steep in people with for example, osteoarthritis. As mentioned before the most obvious structure, the ligamentum flavum, can be identified by the rubbery structure of the tissue. In the ideal situation there is a clear 'pop' as the tip of the needle punctures the ligamentum flavum and enters the epidural space. But by for example young adults and pregnant women the spinal ligaments are soft, which makes it hard to identify the different tissues.

In order to localize the epidural space, the procedure continues with the 'epidural space identification'. The most used technique is the loss-of-resistance technique. During this method the anesthetist uses a frictionless syringe filled with saline. This syringe is placed on the needle, which is inserted in the ligaments and the anesthetist applies a pressure on the plunger using his thumb. With the other hand he slowly advances the needle further into the ligaments. The ligaments will not absorb the liquid, in contrast to the epidural space where large amounts of liquid can be injected easily due to the loose matrix of fatty tissue and blood vessels. This causes a sudden loss-of-resistance to the injection of the medium as the tip punctures the ligamentum flavum and enters the epidural space. After the identification is done, the syringe will be removed and the catheter can be inserted, or the analgesia can be injected, depending on the kind of medical interference. Although the epidural anesthesia procedure is not finished at this point, the simulator focusses on training of these steps. The tactile feedback of tissue resistance and the pressure-gradient and -drop are the most important elements of the procedure, which has to be practiced to achieve the required skills.

Tran and Hor et al. [7, 3] performed a research with manual insertion of an 17G epidural needle in porcine subjects which were slaughtered one or two days prior to the tests. This caused dehydration and increased stiffness of the tissue, which led to less realistic measurements. The focus of this research was on the pressure in the needle in combination with the force applied by the thumb of the anesthetist. Since this does not provide clear information about the tissue resistance, this can not be used.

## 1.4 Main objective

The main objective of this research was to provide information about the force- and pressuregradient in the tissue between the skin and the epidural space of a piglet in order to make a realistic simulation of

the force feedback during needle insertion. Therefore the relationship between the force- and pressure gradient and the different tissues (i.e. fat, supraspinal- en interspinal ligaments, ligamentum flavum) was explored. Also the variation in the force- and pressure gradient between piglets and the lumbar and thoracic region has been studied. The most important input values for the simulator and therefore the main questions of the research were; 'What is the required force to puncture the ligamentum flavum?' and 'Is it possible to identify the different tissues by the pressure gradient?'

To determine the appropriate force and pressure values which are required to simulate the force-position and pressure position, measurements with an epidural needle were done. In order to measure these values a medical procedure had to be modified, which caused a hazardous situation given the place of the procedure, near the spinal cord, which is not allowed to perform on humans. Therefore these measurements had to be diverted to animals. Given the anatomical similarities [6] and the experience of the anesthetic lab of the Erasmus Hospital with piglets, the choice was made to use piglets.

## 2 METHODS

### 2.1 Animal research

The force- and pressure measurements were performed on 5 male Yorkshire piglets. The mean weight of the pigs was 41.62 (1.78) kilograms. The entire research phase took place under anesthesia and for muscle relaxation pancuronium bromide (0,2mg/kg/h) was used. After the research the piglets were used by another research group for other tests.

### 2.2 Experimental setup

An epidural needle (BBraun-Perifix, Tuohy, 18G, 80mm) was placed on a measuring device, see figure 2, which was equipped with a force-sensor (FUTEK LLB130) and a pressure-sensor (Honeywell 40PC015G). The force-sensor was placed excentrically, but due to the design this had little or no effect on the force measurements.

In order to track the movement of the needle, both the measuring device and the pigs were supplied with infrared markers. These 6 markers were tracked with 6 camera's of a motion capture system (Qualisys Motion Capture). Both the motion capture and the force- and pressure-sensors were sampled on 200Hz with an USB-2523 data acquisition board (Measurement Computing). The accuracy of the motion capture was about 0.1mm. Besides the 6 motion capture cameras also a digital video camera (Panasonic NV-GS500) was used to capture all tests to create the possibility to visually inspect the insertions afterwards.

Before the experiment started, the piglet was scanned with a CT-scanner. In this way extra information about the anatomy of the spine could be collected. During the scan the piglet was equipped with 3 infrared markers, which stayed in place during the whole experiment. Although a constant insertion velocity was preferred, the needle was introduced manually into the ligaments. Since the measurements were performed on living animals and automated insertion of the needle is very difficult, due to anatomical variation, manual insertion was chosen.

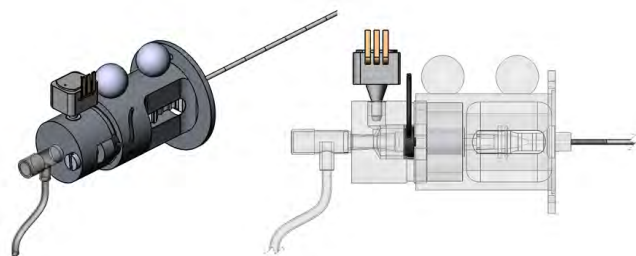


Fig. 2. Measuring device to measure pressure in- and force on the needle, with on top two markers for motion tracking.



To ensure consistency in the compression process the APAD EL (Equip Medikey) was used for the epidural indentation instead of the loss-of-resistance technique. This apparatus was connected to a standard IV-pump with a flow of 100ml/h of Lactated Ringer's solution and gave visual and auditory feedback on the pressure in the needle. More information about the APAD can be found in Appendix A. Due to the pressure measurements in the needle the insertions took place without a stylet in the epidural needle.

Before the insertion started, the insertion area was checked by ultrasound (MicroMaxx - SonoSite), to determine the right insertion angle and to estimate the depth of the ligamentum flavum. After the identification by the APAD, the identification was confirmed by an ultrasound inspection of the epidural space, where Lactated Ringer's solution was injected to confirm the place of the needle tip. The injection of Lactated Ringer's solution was done by an extra syringe which was connected to the measuring device, figure 2, by a Y-split where one side was connected to a separate syringe filled with Lactated Ringer's solution and the other side was connected to the APAD. This enabled the APAD to remain connected to the measuring device during the audit in order to minimize disruption of the needle. Extra information about the setup can be found in Appendix B.

### 2.3 Procedure

The needle was inserted between as many vertebrae as possible, which due to anatomical limitations resulted in 12 levels (Th9-Th10 until L5-L6), see figure 2 and Appendix G. Per level the needle was inserted with respectively the midline-, paramedian left- and paramedian right approach, resulting in 180 measurements. Per piglet, one epidural needle was used, with the needle tip pointed in cranial direction. The insertion places were determined by anatomical landmarks and ultrasound and subsequently marked with a permanent marker on the back. Prior to the measurements the skin at all the insertion places was removed up to 3 mm in depth by a biopsy punch ( $\varnothing 3\text{mm}$ ), in order to prevent that the needle sharpness would be influenced too much by the rigid skin. The order of insertions at different levels was randomized so the effects of wear of the needle was smoothened.

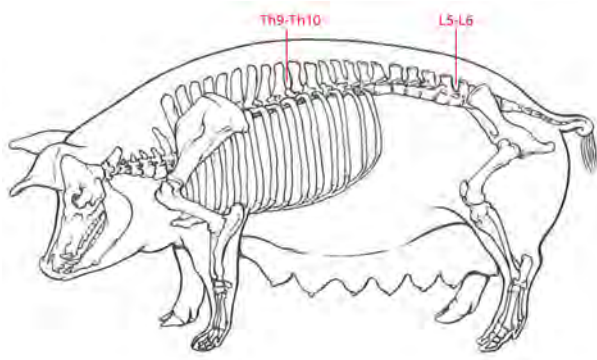


Fig. 3. Skeleton of a pig with the start and end of the insertion places. Adapted from [5]

The manual insertion of the needle was done by an experienced (500+ procedures) anesthetist. Before the measurements on living piglets, the anesthetist practiced on 5 already sacrificed piglets, to get familiar with the anatomy of a piglet and to keep the learning curve of this outside the measurement results. Events during the measurements such as bone contact and incorrect insertion paths were recorded through a switch board which was sampled along the other sensors. This was also the case with the indication of successful or aborted measurements. When during a measurement more than 7 bone contacts occurred, the test was aborted. During the tests the observations of the anesthetist, such as difficult or even remarkably well insertions, were written down.

As described in the experiment setup paragraph, the epidural space identification by the APAD was confirmed by an ultrasound inspection of the epidural space, where Lactated Ringer's solution was injected to confirm the place of the needle tip.



Fig. 4. Photo of a test subject. Visible are the different insertion sites where the skin is removed, with above insertion level 11 the marker of the motion capture system.

### 2.4 Data analysis

To obtain the displacement of the needle, the unitvector of the two markers on the needle were determined. With the known dimensions of the measurement device the place of the needle tip could be calculated. Another marker which was placed 1 cm above the 'paramedian right' insertion place was used to calculate the insertion places. This marker, which can be seen in figure 4, was replaced when another level was punctured. If during the measurements more than 7 times bone-contact of wrong insertions occurred, the results were ignored during the analysis. Also if the anesthetist suspected that he had reached the epidural space via bone, the test results were excluded. A few examples of the collected data are given in figure 5. The most important force event during the needle insertions is the tissue-resistance of the ligamentum flavum. This event can be found in the force-time data in the peak-force in the vicinity of the pressure-drop. The force-peaks were obtained from the measurement data by an algorithm which scanned the force data starting from an insertion depth of 30 mm. This excluded the force-peaks which eventually occurred by puncturing the supraspinous ligament. The algorithm started after the last bone-contact or incorrect insertion path. The moment of pressure drop was found by scanning for the peak-pressure. At the moment the needle tract comes in an open connection with the epidural space, the pressure in the needle drops immediately. By obtaining the pressure-peak this moment is found.

Given the nature of the data with only positive values for the peak-force, a right skewed distribution of the peak-force data could be expected. The data was transformed to a normal distribution by a  $\log_{10}$  of the data. The mean and the standard deviation of the  $\log_{10}$  distribution was back transformed to obtain the geometric mean ( $\bar{x}^*$ ) and the multiplicative standard deviation ( $s^*$ ).

## 3 RESULTS

### 3.1 Force-variation

The measured peak-forces can be described with a lognormal distribution with a geometric mean of 7.754 N with a multiplicative standard deviation of  $(\bar{x}^*)1.423$  N. More information about the transformation can be found in Appendix E.

#### 3.1.1 Force-variation between piglets

Figure 6 shows the variation in peak-force per piglet. The peak-force is indicated in the raw data with the red circle in the force-graph, see figure 5. The data is presented in boxplots; the red line is the median,

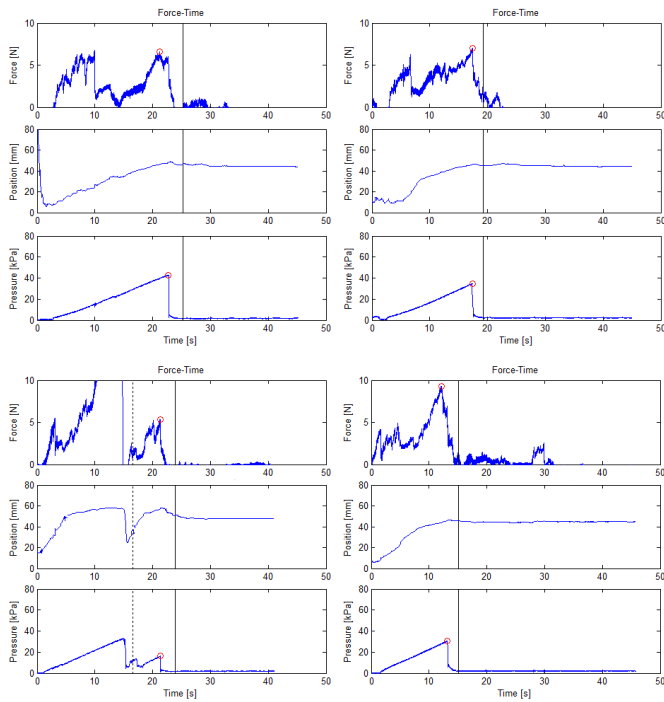


Fig. 5. Raw data of four measurements. Upper graph shows the measured axial force, the middle shows the displacement of the needle tip with respect to the skin and the lower graph shows the measured pressure in the needle. The red circle in the force graph indicates the analysed force-peak. The red circle in the pressure graph indicates the analysed pressure-peak. The black line indicates the moment that the identification was confirmed. The dashed line in the third graph (bottom left) indicates a bone-contact.

the edges of the box are the 25th and 75th percentiles and the whiskers extend to the most extreme datapoint within 1.5 times interquartile range of respectively the first and third quartile. The data outliers are marked with a red cross. The bone-contacts within each testsubject are shown above each boxplot. The boxplots of the measured data between the pigs show that the force differences are small. This fact and given the sample size of the data shows that there is no systematic difference between the piglets.

Due to the fact that the needle sharpness influences the peak-force needed for cutting the ligamentum flavum and given the number of bone-contacts during the measurements, the needle tips were visually inspected. In figure 7, the needle tips are shown with a 25X magnification. The damages are indicated with the black arrows. Notable is that in the measurements with the needle tips with visible damage also a slight increase in the median value can be observed.

### 3.1.2 Force-variation between vertebra

The other points of interest were the differences in force-peaks in the between vertebrae comparison. In figure 8 the boxplots of these values are shown. Surprising are the big differences in spread of the data. There could be expected that differences in peak forces between the thoracic and lumbar vertebrae could be observed due to differences in anatomy of the vertebrae. However, no clear correlation is seen between thoracic vertebrae compared with the lumbar vertebrae.

### 3.1.3 Average insertion speed

An interval was taken of the measured position of the needle with respect to the back of the pig, to neglect the retraction movements. Only the interval with the last inward movement from 30 mm depth insertion to the depth where the pressure drop took place was used. An

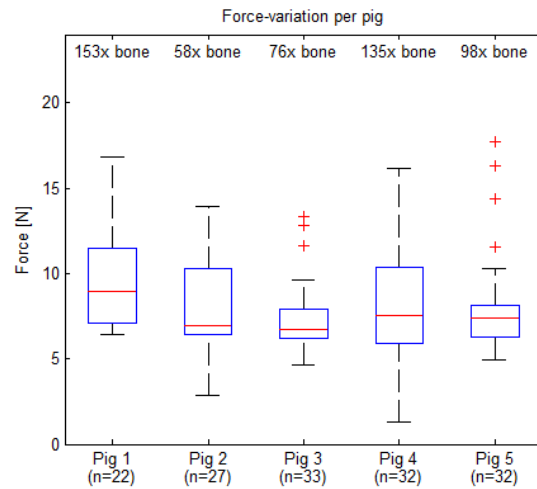


Fig. 6. Force variation per piglet with in the top of the graph the bone-contacts per test.

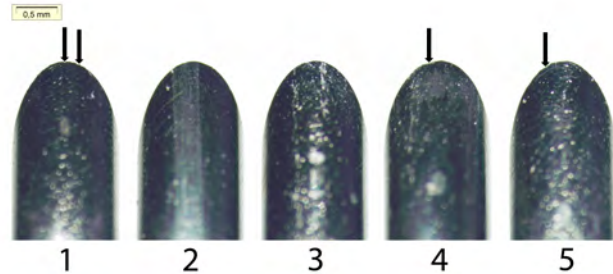


Fig. 7. Needle tips photographed after the experiments with the arrows indicating the visually observable damage.

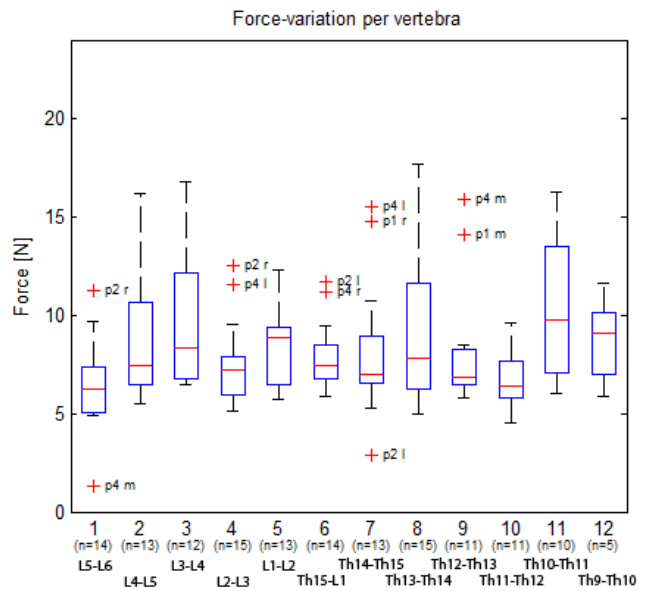


Fig. 8. Force variation between the different insertion places.

approximation of the average insertion speed was made by dividing the covered distance by the time between these two points. The re-

sult can be approximated by a normal distribution with a speed of 2.0 mm/min ( $s=0.86$ ).

### 3.2 Pressure-variation

The pressure-peaks which occurred before the pressure drop were collected to search for relationships in this data. Examples of these peaks can be found in figure 5, where these peaks are indicated with a red circle. The pressure peaks of all measurements were normally distributed with an mean of 35.77 KPa ( $s=11.31$ ).

#### 3.2.1 Pressure gradient

Since the pressure graphs, as showed in figure 5 suggests that the pressure build is time dependent, this was further explored. During the experiments an occlusion test of the needle was done while the pressure was measured. This showed a pressure build-up with a slope of 1.96 KPa/s. In order to verify this with the measured values the pressure data from tests with only an inward movement of the needle was used ie. where no bone-contacts or wrong insertions occurred. An interval was taken from the moment that 10 KPa was reached until the moment of the pressure peak. The duration of interval was plotted against the reached peak pressure. This graph is shown in figure 9. Also the pressure build-up of an occluded needle was plotted in the figure.

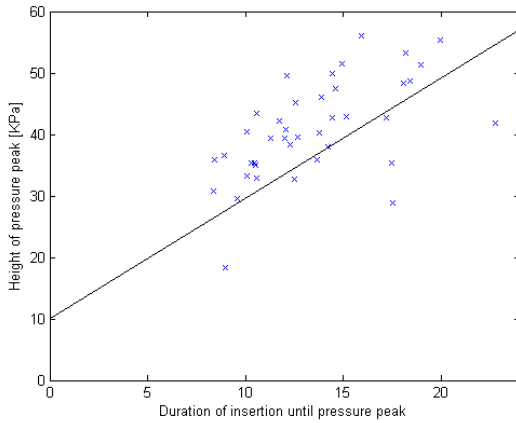


Fig. 9. Duration of the insertion from 10KPa until pressure-peak. The black line represents the measured pressure build-up in an occluded needle.

Besides also the slope of the pressure gradients in two test were checked. These are plotted together with the slope of the occluded needle in figure 10.

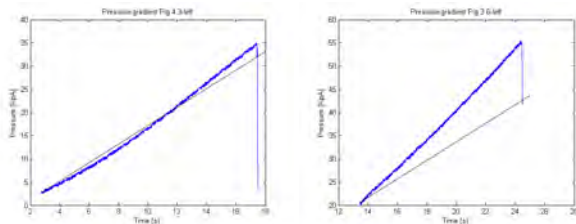


Fig. 10. Pressure gradient in respectively test 'Fig 4, L3-L4, paramedian left' and 'Fig 3, Th15-L1, paramedian left'. The black line represents the measured pressure build-up in an occluded needle.

### 3.3 Differences in force-peak vs. pressure-drop

The distance between the place of the force-peak versus the place of the pressure-drop were compared for paramedian left,- right and midline. These results are presented in a boxplot, see figure 11, where

a positive value represents the occurrence of the force-peak before the pressure-drop, in contrast to a negative value where the events occur in a reverse order. The mean of all distance data is 1.17 mm ( $s=1.217$ ).

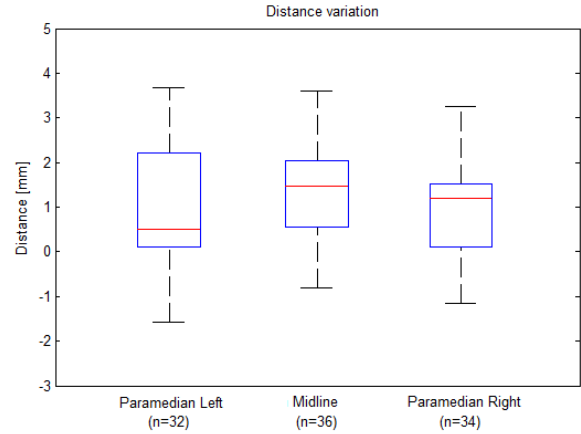


Fig. 11. Variation in distance between the pressure-drop and the force-drop.

## 4 DISCUSSION

Collecting force and pressure data from living tissue is very difficult. It is hard to prove in which tissue layer the measurement takes place, with as result that only very obvious events can be used. In this case the force-peak and pressure-drop are very clear indicators of the ligamentum flavum. Therefore some statements about these values can be done.

### 4.1 Force data

There is no clear difference in the force data in the between subjects data. The force gradient is influenced by the manual insertion of the needle, therefore the force-position data can only be used near the ligamentum flavum where than needle position has only an inward direction. This makes it very difficult to make statements about the force in combination with fat-, supraspinous-, and intraspinous tissue.

In the force-peak data a slight higher median can be found in the experiments were a high number of bone-contacts occurred. Although it can not be said with certainty, this could be due to the visually detectable damage of the needle tips. This is likely because the dulling of the tip has direct impact on the measured axial forces.

What is remarkable is the lag of difference in force-peaks between the insertion at thoracic (7-12 in figure 8) and lumbar level (1-5 in figure 8). Due to the anatomical differences of the vertebrae it could be expected that there would be a difference. This fact simplifies the simulation of the different insertion levels.

The similarities in force-peaks with the midline, paramedian right and paramedian left approach were as expected; no systematic difference in peak-force at different angles. It is not very surprising that the angle of approaching the tissue has little effect.

### 4.2 Pressure data

In the pressure-time data could be seen that the pressure build-up is mainly time dependent. Since there is also position data, this could give information about the 'absorption' capacity of the different tissue and border areas between the tissues. But since the needle insertion happened manually with a non constant insertion velocity as result, the data must be corrected for the velocity.

Given the time-dependence of the pressure-data the height of the pressure-peak which was selected out of the data is only an indication of the duration of the insertion. Surprising are the results for the height of the pressure peak with respect to the duration of the insertion. It could be expected that the values would be below the slope of

an occluded needle, but the opposite is the case. The same can be seen in the comparison of the two pressure gradients with the slope of the occluded needle. Perhaps the tissue which is pressed into the needle tract during the needle insertion performs the pressure boost. Before firm statements can be made, first the pressure build-up with respect to the insertion speed should be viewed. Also a second occlusion test would be preferred, since the occlusion test used was only 5 seconds long.

Although the pressure build-up is not totally clear this is not a big issue for the simulator. During exercise of the loss-of-resistance technique, only the last millimeters of the insertion are done with pressure feedback, where the pressure-drop is most important event.

### 4.3 Needle tip position

Despite the high accuracy of the motion capture system it is difficult to prove with certainty in which tissue the needle tip is located. The marker on the back of the piglet was manually replaced when the measurement was moved to another level. This creates inaccuracy in the approach of the insertion place in the motion capture data. Given the distance between the needle tip and the skin of the pig this inaccuracy can be neglected around the ligamentum flavum, due to the distance between the needle tip and the insertion place. The inaccuracy of the motion capture does not influence the depth measurement of the needle, only the position of the needle on the measured depth. In the raw-data this inaccuracy can be found in the displacement graph, which does not start at 0. This is a combination of the start place of the insertion, which is due to the skin removal at 3mm, and the inaccuracy of the manual placement of the marker. The displacement graph shows the absolute distance between the needle tip and the insertion place.

### 4.4 Distance between force and pressure events

An explanation for the difference in the force-peak before or after the pressure-drop may lie in different phases of the puncture. It seems

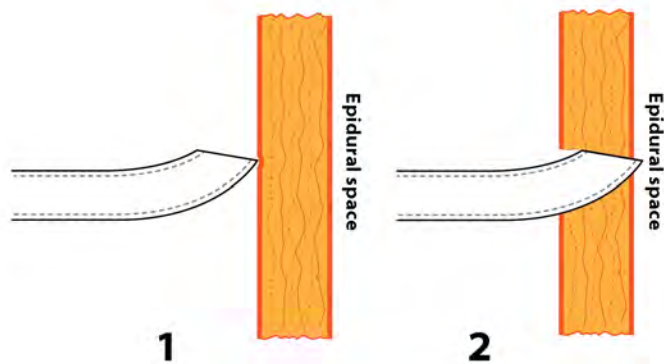


Fig. 12. Different phases in needle-tissue interaction. 1. Pre-puncture (Tissue boundary displaced but still intact; 2. Tip breakthrough (Needle canal in contact with epidural space)

that when the peak force occurs early, it is due to the pre-puncture or tip-insertion phase, but on the other hand with a late occurrence of the peak force, after the pressure drop, it can be assigned to the tip breakthrough phase. The pressure drop occurs at the moment the tip of the needle enters the epidural space and the channel of the hollow needle is connected to the epidural space. At that moment the curved tip of the needle is still in the ligamentum flavum. As can be seen in figure 13, where the dimensions of the needle tip are given, it is plausible that the insertion of the curved tip can cause a tearing force at 1.5 mm after the pressure drop. Although it might be expected that in the force-event vs. pressure-event data differences would appear between paramedian or midline insertions, given the difference in approach of the ligamentum flavum, this is not visible in the data. This suggests that the difference can be dedicated to the discontinuity of biological tissue. Important to mention is the manner of peak selection. In figure

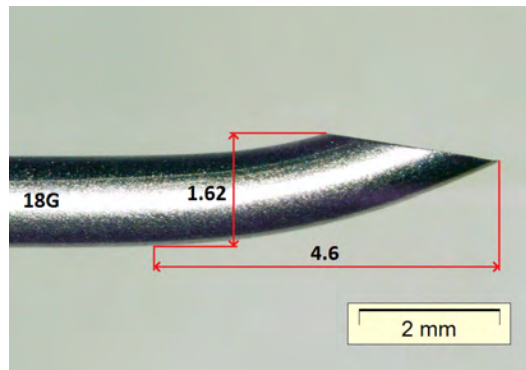


Fig. 13. Needle sizes; 18G BBraun epidural needle.

5 it can be seen in the first and the third measurement that two high peaks are present. Most probably these two peaks can be dedicated to the two insertion phases as described in the results. From these two peaks only the highest was taken into account. Although this measurement is difficult to interpret, it is an important value in simulating the ligamentum flavum.

### 4.5 Other observations

Another interesting result is similarity in the order of magnitude of the peak-force in live vs. dead tissue. Although this research did not focus on difference in tissue between live vs. dead biological tissue, it is interesting to see the force-peaks of the pilot test which was performed on an already offered male Yorkshire piglet, with a decay-time of 1-5h. During the pilot test the measurements were performed on 10 levels (Th11-Th12 until L5-L6), in total there were 30 measurements which were treated the same way as the real tests. The measured peak forces are in the same range as live tissue. Without making firm conclusions, this could mean that no living pigs have to be used for measurements, to obtain reliable force-feedback of the ligamentum flavum.

### 4.6 Validity of pig model

The question arises in what extent the pig model is suitable as input for the simulation of human spine. The spinal column of a pig is situated in a horizontal position, while that of humans is vertically positioned, so that these have to deal with a complete different moment lines. This is also reflected in the comparison of the vertebrae, the spinous processes (the protuberances at the outside) in the thoracic region of the vertebral column of a pig are much larger than is the case in humans. However during the experiments the anesthetist noticed several times that the specific test did exactly felt as in humans. Given the lack of systematic differences in peak-forces between the vertebrae of the pig does suggest that the pig model is a reliable alternative.

## 5 CONCLUSION

The questions that led to this research were; 'What is the required force to puncture the ligamentum flavum?' and 'Is it possible to identify the different tissues by the pressure gradient?'

The outcome of this research is that the force needed to penetrate the ligamentum flavum with a 18G epidural needle can be described by an lognormal distribution and lies in the 68.3% confidence interval of 5.45 till 11.03 N and has an geometric mean of 7.754 N. The experimental results showed that there is no systematic difference in force peaks between piglets and neither between vertebrae.

Another interesting observation was that the force-peaks measured in deceased tissue (1-5h) are in the same range as the force-peaks in living tissue.

The measured pressure data showed that the pressure gradient is time-dependent when using a constant flow of liquid, although another factor causes that the pressure builds up more quickly. Further exploration of this data will have to be done before valid statements can be made about the pressure build-up. Based on the current observations it

is most probably not possible to identify the different tissues on basis of the pressure gradient.

The distance between the peak-force event and the pressure-drop event can be described by a normal distribution 1.17 mm ( $s=1.217$ ), where a positive value means that the force event occurs before the pressure-drop.

The experimental results can be used to make a more lifelike simulation of the epidural anesthesia procedure and thereby improving the safety of the patient.

## REFERENCES

- [1] P. N. Brett, T. J. Parker, a. J. Harrison, T. a. Thomas, and a. Carr. Simulation of resistance forces acting on surgical needles. *Proceedings of the Institution of Mechanical Engineers, Part H: Journal of Engineering in Medicine*, 211(4):335–347, Apr. 1997.
- [2] A. M. Dogliotti. Segmental peridural spinal anesthesia. A new method of block anesthesia. *The American Journal of Surgery*, 20(1):107–118, 1933.
- [3] K.-W. Hor, D. Tran, A. Kamani, V. Lessoway, and R. Rohling. Instrumentation for epidural anesthesia. *Medical image computing and computer-assisted intervention : MICCAI ... International Conference on Medical Image Computing and Computer-Assisted Intervention*, 10(Pt 2):918–25, Jan. 2007.
- [4] C. Konrad, G. Schüpfer, M. Wietlisbach, and H. Gerber. Learning manual skills in anesthesiology: Is there a recommended number of cases for anesthetic procedures? *Anesthesia and Analgesia*, 86(3):635–639, 1998.
- [5] W. Sack. *Essentials of pig anatomy - Horowitz/Kramer atlas of musculoskeletal anatomy of the pig*. Veterinary Textbooks, 1982.
- [6] M. Swindle and A. Smith. Comparative anatomy and physiology of the pig. *Scand J Lab Anim Sci*, 25(Suppl 1):1–10, 1998.
- [7] D. Tran, K. W. Hor, A. A. Kamani, V. A. Lessoway, and R. N. Rohling. Instrumentation of the loss-of-resistance technique for epidural needle insertion. *IEEE Transactions on Biomedical Engineering*, 56(3):820–827, 2009.

Appendices belonging to the Masters thesis:

Force and pressure feedback during  
epidural needle insertion in the  
ligamentum flavum of piglets.

W. Boessenkool

# CONTENTS

<b>A</b>	<b>Introduction in Epidural Anesthesia</b>	<b>3</b>
A.1	Anatomy of the human vertebral column . . . . .	3
A.1.1	Procedure of epidural anesthesia . . . . .	5
A.1.2	Equipment used during epidural anesthesia . . . . .	5
A.2	Techniques used for epidural space identification . . . . .	7
A.2.1	The Loss of resistance technique . . . . .	8
A.2.2	The Hanging drop technique . . . . .	8
A.2.3	APAD . . . . .	9
<b>B</b>	<b>Experimental Setup</b>	<b>12</b>
B.1	Qualisys motion capture . . . . .	12
B.2	Measurement device . . . . .	12
B.3	Additional tools . . . . .	13
B.4	Animal preparation . . . . .	13
B.5	Images . . . . .	14
<b>C</b>	<b>Experiment protocol</b>	<b>22</b>
C.1	Prepareren varken . . . . .	22
C.2	Motion Capture . . . . .	22
C.3	HD Camera . . . . .	23
C.4	Sensor Unit . . . . .	23
C.5	APAD . . . . .	23
C.6	Draaiboek epiduraal punctie . . . . .	24
C.7	Het prikken . . . . .	25
C.8	Invulformulieren . . . . .	25
<b>D</b>	<b>Results</b>	<b>26</b>
<b>E</b>	<b>Statistics</b>	<b>33</b>
E.1	Transformations . . . . .	33
E.1.1	Without transformation . . . . .	33
E.1.2	Natural logarithmic transformation . . . . .	33
E.1.3	Common logarithmic transformation . . . . .	33
E.1.4	Square root transformation . . . . .	33
E.1.5	Square transformation . . . . .	34
E.1.6	Twice the common logarithmic transformation . . . . .	34
E.1.7	Reciprocal transformation . . . . .	34
E.1.8	Descriptive statistics . . . . .	34

<b>F</b>	<b>Data analysis</b>	<b>39</b>
F.1	Qualisys . . . . .	39
F.2	Matlab . . . . .	40
<b>G</b>	<b>CT-scan</b>	<b>43</b>



## INTRODUCTION IN EPIDURAL ANESTHESIA

The discovery of anesthesia was an important milestone in the development of the modern civilization. Improvements were made gradually during the ages and in 1933 the first publication about 'peridural anesthesia', nowadays known as epidural anesthesia, was made by prof. A.M.Dogliotti (2).

With epidural anesthesia a local anesthetic block can be applied, which has great benefits compared to total anesthesia. The greatest impact epidural anesthesia had was in obstetric anesthesia; cesarean section is most commonly performed under epidural or spinal anesthesia and epidural anesthesia is widely used for analgesia in women during vaginal delivery of the baby. Both blocks, spinal and epidural, allow a mother to stay conscious and experience the birth of her child.

### A.1 Anatomy of the human vertebral column

The spinal cord of the human body contains nerves coming from and going to the brain. They can be separated in motor nerves, for actuating the muscles and organs, and sensory nerves for feedback. When blocking the nerves which conduct information leading to the perception of feeling, the brain does not detect that something is wrong. For example, this technique is used during

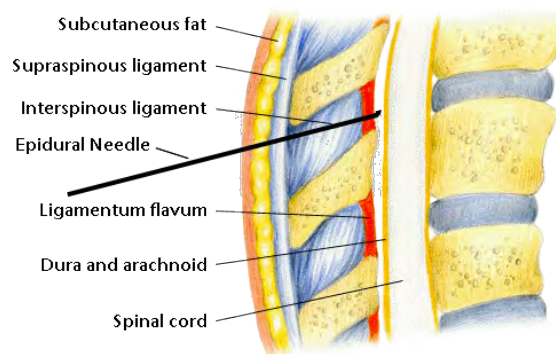


**Figure A.1:** Epidural anesthesia, with needle tip present in the epidural space.

surgery. Because the sensory nerves which detect pain are smaller in diameter than the sensory nerves which give feedback from the organs, these are more easy to block than other feedback nerves. Neuraxial anesthesia, anesthesia around the nerves of the central nervous system, can be split up in spinal and epidural anesthesia. Spinal anesthesia is the blocking of nerves in the spinal cord itself and epidural anesthesia is the blocking of the spurs in the epidural space.

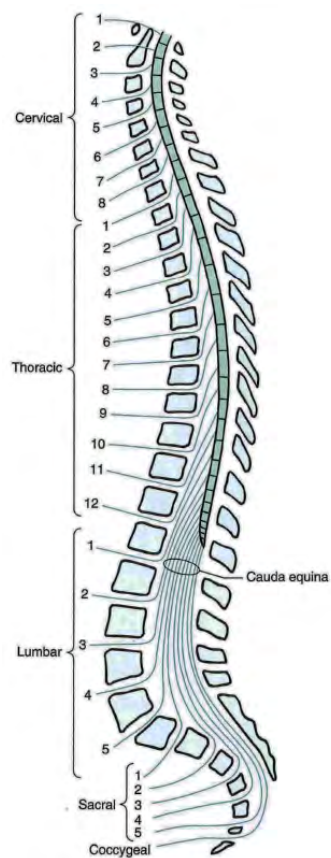


**Figure A.2:** Human vertebral column. (3)

The spinal cord is protected by the meninges (resp. dura mater and arachnoid) and the space around (epi) the dura mater is called the epidural space.

When injecting analgesia in the epidural space, only the spurs from the spinal cord are blocked, and as a result the nerves going to body parts below the place of injection are still normal. This is not the case with spinal anesthesia, where everything below the place of insertion is blocked.

In order to get to the epidural space, the needle has to penetrate skin, muscles and ligaments, which is done with tactile feedback. This demands an extensive skill of interpreting the forces due to resistance of the tissues. In extreme cases such as obese patients or patients with shrunken spines due to osteoporosis, it is very difficult to perform. The most obvious structure, the ligamentum flavum, can be identified by the rubbery structure of the tissue. In young adults and pregnant women the spinal ligaments are soft, which makes it hard to identify the different tissues. After entering the epidural space the advancement of the needle has to be stopped to avoid overshoot, which can result in puncturing the meninges (dural tap) and nerve damage in the spinal cord. The risk on spinal cord damage depends on the place of the needle insertion at the vertebral column, which will be explained later in this chapter.

In medical jargon, the naming of the vertebral column is divided into four parts, respectively cervical, thoracic, lumbar and sacral.

The place of needle insertion depends on the medical interference that has to be done. The epidural blocks in the cervical and thoracic region are the most hazardous, due to the fact that in this region the spinal cord consists of compact nerve tissue, which will be damaged when it is penetrated during an overshoot. This is different from the lumbar and sacral region, where the spinal cord has proceeded to the cauda equina, which is a collection of nerve spurs at the bottom

of the spinal cord. When the meninges in this region are accidentally punctured, the possibility of nerve damage is by far smaller because the needle is able to pass easily between the spurs.

1

### A.1.1 Procedure of epidural anesthesia

The first part of the penetration is always done on tactile feedback. The anesthetist determines between which vertebral disks and in what angle the needle has to be inserted. The angle of insertion depends on the position of the vertebrae, which can be quite steep in people with for example osteoarthritis.

In the ideal situation there is a clear 'pop' as the tip of the needle punctures the ligamentum flavum and enters the epidural space, but especially in pregnant women and young adults, the ligaments are soft with a less obvious 'pop' as a result, which causes the identification to be difficult. In order to still identify the epidural space the anesthetist is required to do an extra action; when he thinks that the epidural space is almost reached, he can choose between several techniques to identify the epidural space, the so called epidural space identification (ESI) techniques.

Epidural anesthesia can be difficult to perform and may be time-consuming. It depends on the patient's physical characteristics (such as age, arteriosclerosis, pregnancy, venous circulation and extradural fat) as well as the anesthetist factors (positioning of the patient, choosing the site of epidural puncture, orientation of the needle bevel, determining the speed of injection, volume and concentration of the anesthetic solution) (14). In cases where the identification is presumed to be difficult, it is possible to identify the epidural space with the use of imaging techniques before the penetration, so the anesthetist is able to make an assumption of the penetration depth of the needle. This was also done before each measurement on the piglets.

### A.1.2 Equipment used during epidural anesthesia

The epidural needle is typically 16-18 Gauge (1.65-1.27mm), and is 5, 8 or 15 cm long, depending on the type of patient. The most commonly used needle is the Tuohy needle, which has an 15-30

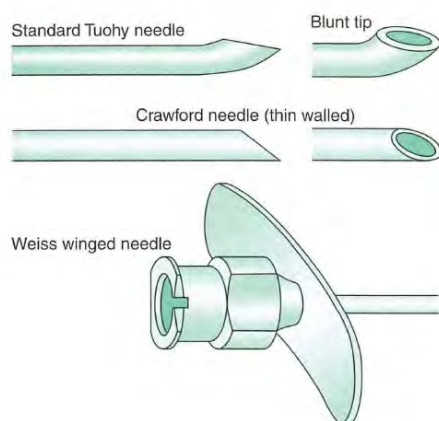


**Figure A.3:** Epidural Needles; Tuohy needle (above), Crawford needle (middle) and the needle wings (below). (3)

degree curved tip to help prevent puncture of the meninges (3), see fig. A.3. The hollow needle is filled with a stylet, to prevent tissue obstructing the needle. Before applying an ESI technique, the stylet has to be removed.

<sup>1</sup>The anatomical information discussed in this chapter primarily comes from the book Clinical Anesthesiology, Edward Morgan, and cited literature and was completed by supervisor Mark Vogt.

The block can be performed with the patient in a sitting or laying position (lateralis decubitus). Preferable the patient has a curled up position, as this enlarges the space between the spinous processes of the vertebral discs and simplifies the identification of the intervertebral spaces.

There are two types of approaching the epidural space, resp. the midline and the paramedian approach, see fig. A.4. Normally the midline approach is used, but the paramedian approach may be selected when the epidural block is different, due to arthritis, kyphoscoliosis, or prior lumbar spine surgery. The paramedian approach offers a much larger opening into the spinal canal than the midline approach, but because this approach is lateral to most of the intraspinal ligaments and paraspinal muscles the feeling is totally different. The identification of the ligamentum flavum and the pressure drop in the epidural space with the loss of resistance method are more subtle than with the midline approach (3). In order to provide continuous epidural analgesia,

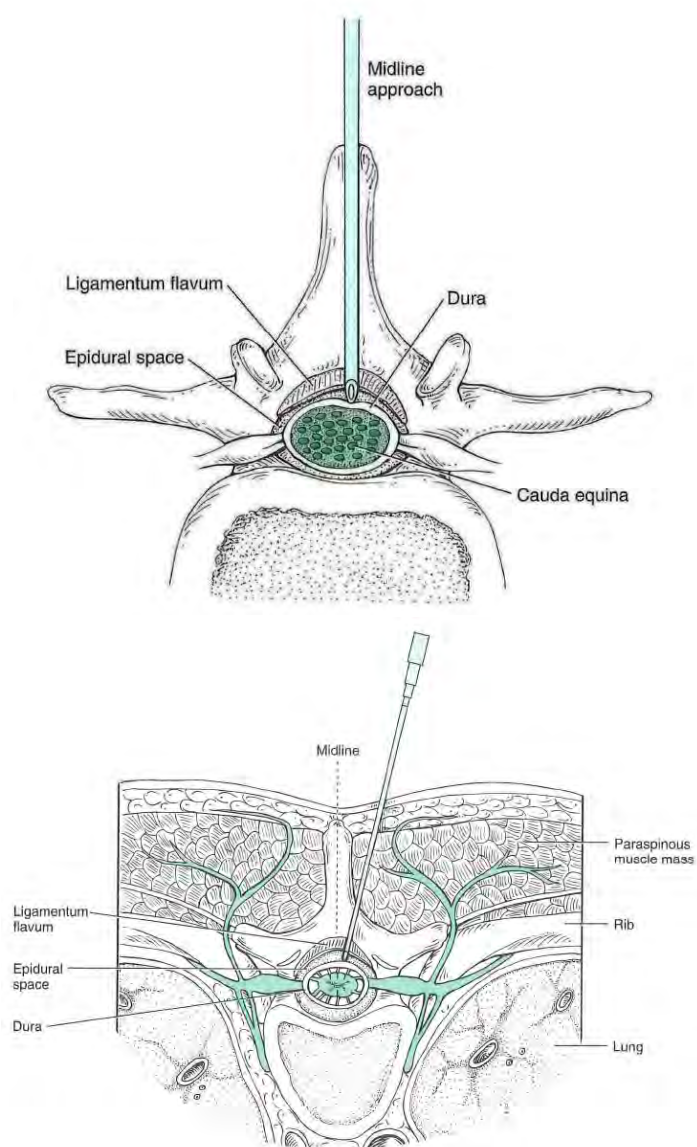


**Figure A.4:** Midline (left) and paramedian approach (right). (3)

a small hollow catheter could be conducted through the hollow needle into the epidural space

and left there while the needle is removed. After checking if the catheter did not puncture any blood vessels, by aspirating a small amount of fluid from the catheter, the anesthetist administers analgesic fluid. With a failed identification of the epidural space, the analgesia will fall short, and epidural anesthesia has to be performed again. An overview of the different steps in the procedure can be found in fig. A.5. The red box marks the focus of the research in this thesis.

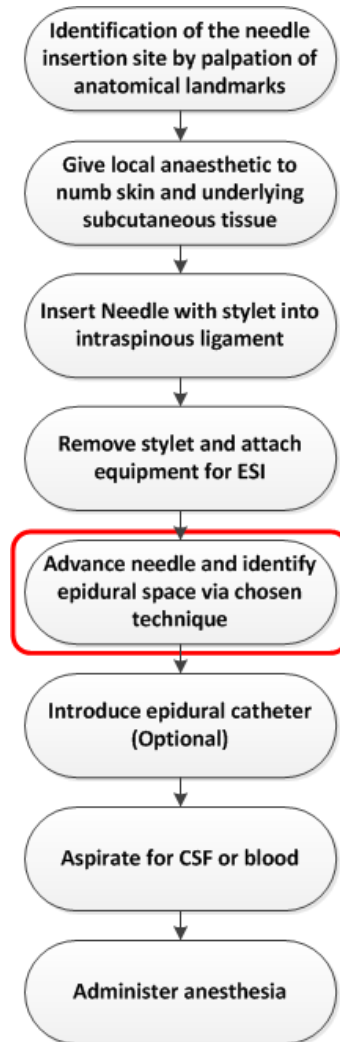


**Figure A.5:** Overview of the different steps in the Epidural Anesthesia procedure.

## A.2 Techniques used for epidural space identification

During epidural space identification, several methods can be used. The most common methods are the "loss of resistance" method (LOR) and the "hanging drop" method (HD). Especially the LOR method is widely used.

During insertion of the needle, the use of both hands is desirable, in order to achieve as much control over the penetration as possible and to improve the haptic feedback of the small changes in resistance. Especially in small children where the epidural space can be found 1 centimeter below the skin, it is important to have as much control as possible.

The ESI is extra important while applying under total anesthesia due to the fact that with a

misapplied insertion, the consequences are not directly visible. ESI techniques like LOR and HD have proved to be safe when managed well, although improvements can be made.

### A.2.1 The Loss of resistance technique

For this method the anesthetist uses a frictionless syringe filled with saline (or less often a local anesthetic), air or a mixture of both. This syringe is placed on the needle, which is inserted in the ligaments and the anesthetist applies a pressure on the plunger using his thumb, see fig. A.6. With the other hand he slowly advances the needle further into the ligaments. The ligaments will not absorb air or liquid in contrast to the epidural space where large amounts of liquid or air can be injected easily due to the loose matrix of fatty tissue and blood vessels. This causes a sudden loss of resistance to the injection of the medium as the tip punctures the ligamentum flavum and enters the epidural space.

The procedure is done with two hands, as one is advancing the needle into the spine the other hand is putting intermittent or continuous pressure on the plunger of the syringe.

The best media for the LOR-technique, fluid or air, is a controversial subject, about which sev-

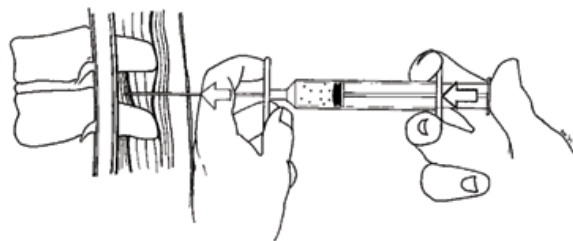


**Figure A.6:** Loss of Resistance technique.

eral studies have been done. Both the medical effects (11) as the physical effects (5; 13) on the perception of the identification, have been studied, by which fluid was usually assessed best.

An advantage of using a fluid is that it provides a better proprioception due to its incompressible behaviour. However, using air provides an easy identification of a sticky syringe plunger. Also both media have disadvantages, the use of saline is known to dilute and decrease the effect of the local anesthetic, whereas epidural injection of air carries several risks (6; 10). When an anesthetic solution is used instead of saline, there is a risk that the solution ends up in the wrong place, for example in the spinal area in case of a dural tap.

In the ideal situation the LOR technique is a good technique for identifying the ES, but with a needle insertion into a blood vessel, subarachnoid space (a space between the two meninges which can occur) or a hole or cyst in the interspinous ligament (12) can give a false identification.

### A.2.2 The Hanging drop technique

The fact that in the epidural space a negative pressure prevails, is used in this technique. Alberto Gutierrez was the first one who noted the disappearance of a drop of fluid hanging from the hub of the needle during insertion of this needle into the back of a patient (1). His first publication about the hanging drop was in 1933. Unfortunately there is little literature available about the HD-technique.

After inserting the needle into the ligaments, the stylet is removed and the needle is filled with liquid using a syringe, after which the syringe is removed. The needle, which is filled with liquid in a way that a drop is hanging outside of the end of the needle, is slowly pushed into the tissue, see fig. A.7. As long as the needle remains within the ligamentous structures, the drop is hanging at the end of the needle. As soon as the tip of the needle reaches the epidural space, the drop of fluid is aspirated into the needle due to the negative pressure. When the needle is advanced too

far, it punctures the meninges, with free flow of liquor from the dural sac as result. The flow of liquor out of the needle is a very important indicator that the needle is pushed too far and the penetration has to stop immediately. The hanging drop is a technique which is only reliable in the cervical and thoracic section of the vertebrae due to the negative pressure which is only available in those regions (14).

A disadvantage of the HD method is that it sometimes yields 'false-negative' results, in other words the drop is not aspirated even when the needle tip is present in the epidural space. This can be on account of needle obstruction, but also because of anatomical abnormalities. Due to the fact that the technique is used in the thoracic region, this is not without danger. Another disadvantage of the HD-technique is the fact that it can only be done once, for the pressure difference disappears after the needle punctures the ligamentum flavum and an open air connection is made. This means that after failed catheter placement, another technique has to be used to do a new identification.

In the thoracic region the passage between the vertebral disks is very steep and long. Therefore

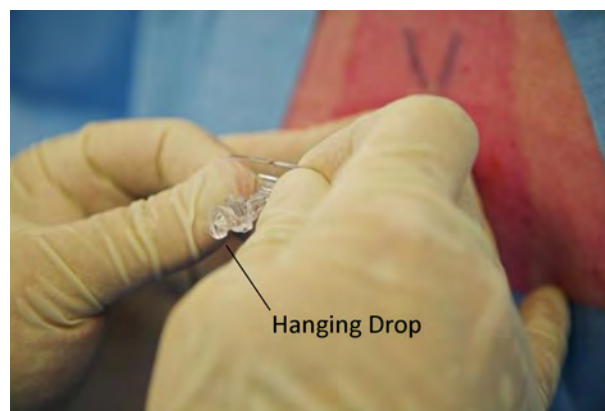


**Figure A.7:** Hanging drop technique (*image source unknown*)

absolute needle control is needed. An advantage of the technique is the hands-on identification, with two hands at the needle, to ensure the control over the insertion.

### A.2.3 APAD

Both techniques do work as identification technique, but both are subjective in their identification. With the LOR technique there is a chance on false positive identification, while with the HD technique is a chance on false negative identification. These techniques have been used for 80 years and during these years there have been some small improvements such as a low resistance syringe instead of a normal syringe, there is however still room for improvement.

Although dural taps only occur at around 1.0% of the LOR epidurals, there are also non-registered epidurals which did not work properly due to e.g. a misplaced catheter. As a result these epidurals have to be placed again or, when it shows up during a surgery, total anesthesia has to be administered.

In the search for an ideal identification technique several invention were made. The Acoustic Puncture Assist Device (APAD) is one of them. This technique uses a commonly at hospitals available fluid pump, which is connected to the needle with a small tubing. A pressure sensor in this tubing is connected to the actual device, see fig. A.8. This device converts the pressure into a graph and an acoustic signal. On a screen at the device the graph is updated real-time and the acoustic signal changes from a low to a high sound, resp. low to high pressure. Different from the other ESI-techniques, this technique starts with the needle outside of the ligaments. Since there is a constant flow of saline out of the needle, there is no risk of unnoticed needle obstruction due to tissue. Because the device records the pressure graph, the entire procedure can be observed,

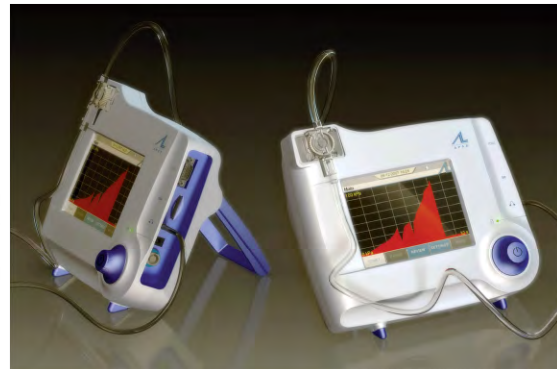
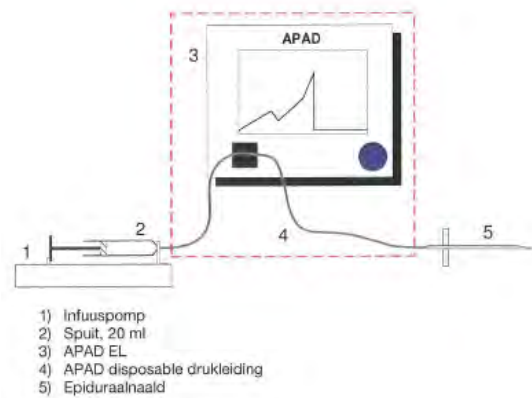


**Figure A.8:** (Left) Schematic view of the APAD. **1** Fluidpomp, **2** Syringe (20 ml), **3** APAD, **4** Disposable pressure tube, **5** Epidural needle (7). (Right) The commercially available APAD Epidural Locator, the red graph represents the pressure on the fluid in the needle (4)

see fig. 3.11. The IV-pump is programmed at a constant speed (100ml/h is been advised by the manufacturer), which ensures that pressure changes at the tip of the needle are due to changes in resistance of the tissue, through which the needle passes. This makes the pressure tracking a reliable indicator for ESI (8). The changes in pressure result in corresponding variations in acoustic and visual signals. This way the passage of the needle tip from tissues of high resistance

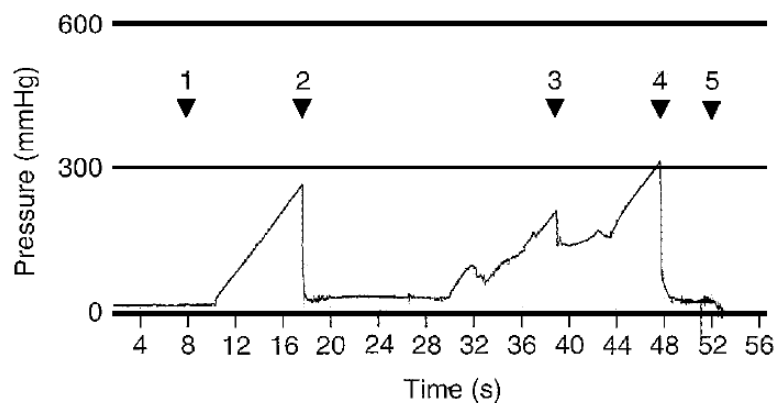


**Figure A.9:** Pressure recording produced by the experimental APAD. **1** Test signal, **2** Start of needle advancement, **3** needle withdrawal because of needle contact to bone and start of repeated needle advancement, **4** a pressure decrease at entering the epidural space and **4 and 5** a low-pressure plateau due to the free flow of saline (9).

(ligamentum flavum) to those of low resistance (epidural space) is made audible and visible. Also the possible existing holes and cysts between the ligaments are made visible with a small dip in the pressure-graph.

A clinical study by the inventor of the APAD, showed on a trial of 100 patients, from which 42 thoracic and 58 lumbar, a score of 100% succeeded ESI (9). Because the pressure at the needle tip is generated by a fluid pump, the anesthetist can use both hands for needle advancement.



## BIBLIOGRAPHY

- [1] Aldrete, J., Auad, O., Gutierrez, V., and Wright, a. (2005). Alberto Gutierrez and the Hanging Drop. *Regional Anesthesia and Pain Medicine*, 30(4):397–404.
- [2] Dogliotti, A. M. (1933). Segmental peridural spinal anesthesia. A new method of block anesthesia. *The American Journal of Surgery*, 20(1):107–118.
- [3] Edward Morgan, G. (2006). *Clinical Anesthesiology - Chapter 16*. Number Spinal, Epidural.
- [4] Equip (2011). [www.equip.nl](http://www.equip.nl).
- [5] Gleeson, C. M. and Reynolds, F. (1998). Accidental dural puncture rates in UK obstetric practice. *International journal of Obstetric Anesthesia*, 7:242–246.
- [6] Laviola, S., Kirvelä, M., Spoto, M. R., Tschuor, S., and Alon, E. (1999). Pneumocephalus with intense headache and unilateral pupillary dilatation after accidental dural puncture during epidural anesthesia for cesarean section. *Anesthesia and analgesia*, 88(3):582–3.
- [7] Lechner, T. J. M. (2009). APAD manual.
- [8] Lechner, T. J. M., Van Wijk, M. G., Maas, A. J., Van Dorsten, F. R., Drost, R. A., Langenberg, C. J., Teunissen, L. J., Cornelissen, P. H., and Van Niekerk, J. (2003). Clinical results with the acoustic puncture assist device, a new acoustic device to identify the epidural space. *Anesthesia and Analgesia*, 96(4):1183–1187.
- [9] Lechner, T. J. M., Van Wijk, M. G. F., Maas, A. J. J., and Van Dorsten, F. R. C. (2004). Thoracic epidural puncture guided by an acoustic signal: Clinical results. *European Journal of Anaesthesiology*, 21(9):694–699.
- [10] Nay, P. G., Milaszkiwicz, R., and Jothilingam, S. (1993). Extradural air as a cause of paraplegia following lumbar analgesia. *Anaesthesia*, 48(5):402–4.
- [11] Schier, R., Guerra, D., Aguilar, J., Pratt, G. F., Hernandez, M., Boddu, K., and Riedel, B. (2009). Epidural space identification: a meta-analysis of complications after air versus liquid as the medium for loss of resistance. *Anesthesia and Analgesia*, 109(6):2012–2021.
- [12] Sharrock, N. (1979). Recordings of, and an anatomical explanation for, false positive loss of resistance during lumbar extradural analgesia. *British Journal of Anaesthesia*, 51(3):253.
- [13] Stride, P. C. and Cooper, G. M. (1993). Dural taps revisited - A 20-year survey from Birmingham Maternity Hospital. *Anaesthesia*, 48(August 1992):247–255.
- [14] Usubiaga, J. E., Wikinski, J. a., and Usubiaga, L. E. (1967). Epidural pressure and its relation to spread of anesthetic solutions in epidural space. *Anesthesia Analgesia*, 46(4):440–446.

## EXPERIMENTAL SETUP

The experimental setup consisted of the measuring device with the pressure and force sensor, the motion capture system and a table.

### B.1 Qualisys motion capture

The camera setup consisted of three tripods, two standing and one horizontal, were the two standing tripods had a T-bar mounted on top of it, see figure B.1 and B.2. The left tripod carried two motion capture camera's and the right tripod carried three camera's. The sixth motion capture camera was mounted above the experiment table with the use of a third tripod. The digital video camera mounted beside the sixth motion capture camera. With this setup always four out of six camera's had full view on the markers.

The motion capture system was calibrated before the experiment started, as described in their manual. The accuracy of the system after each calibration is described in the standard deviation of the calibration wand length, which has a length of 300mm. For the five testdays these accuracies are given in the following table. If during the test the camera's were touched or the system

**Table B.1:** *Calibration accuracy*

Piglet 1	Piglet 2	Piglet 3	Piglet 4	Piglet 5
0.44226mm	0.46361mm	0.54090mm	0.40425mm	0.43204mm

otherwise was influenced, the calibration was performed again. This happened twice, respectively the third and fourth testday. During the data analysis of the motion data this was taken into account. The least accurate measurement used that day is shown in the table in the

Each measurement was 180 seconds long and was sampled on 200 Hz. If the insertion was not completed within 180 seconds, the measurement was aborted.

### B.2 Measurement device

The measurement device was designed and produced by Dennis van Gerwen. An exploded view of the device is given in fig.B.4.

The wings of the epidural needle were removed in order to prevent that touching these wings would influence the measurements. The anesthetist moved the needle with the aim of the wings of the outer sleeve of the device.

The pressure sensor was in direct contact with the APAD and the needle tract.

The force sensor has been adjusted using a screw. The force on the needle was directed by a

tube which was mounted in the device by membranes in order to transmit the axial force on the eccentrically mounted force sensor.

Due to the Lactated Ringer's solution the device was disassembled and cleaned every day to prevent corrosion.

Every day before the measurements the two markers were attached on top of the measurement device in the midline. The distance of the front marker to the front of the device was measured by a caliper and recorded. These values are given in tabel B.2. The way of measuring is given in figure B.5.

A disadvantage of this way of motion tracking of the measurement device is the incapability of measuring the rotation of the device. During the measurements the device was used with the markers upwards and during the data analysis it was assumed that the device was not rotated around its axis during the measurements.

**Table B.2:** *Measured distances*

	Piglet 1	Piglet 2	Piglet 3	Piglet 4	Piglet 5
B	0.75	1.2	2.71	1.9	2.68

### B.3 Additional tools

In order to track the wrong insertions, bone-contacts and successful or aborted measurements an additional input device was made, see figure B.6. The technician used this at the moment the anesthetist verbally indicated that something went wrong or right. When a switch was used a voltage peak of 5 volt appeared in the data, which could filtered out with the use of Matlab. In this manner the data could automatically be interpreted or rejected.

Another additional part was the extra syringe which was attached to the system by an Y-split, see figure B.7. The Y-split did not contain valves.

In this way, fluid could be injected manually during the confirmation of the epidural space by ultrasound inspection, without affecting the needle position or force measurement by replacing the APAD with a syringe. The flow of fluid in the epidural space was visually observable with ultrasound which was used as identification. Every confirmation was captured with the video record function on the ultrasound device.

### B.4 Animal preparation

The piglets were brought in an unconscious state. Then they were lifted on the table and fixed on their back. Two employees of the anesthesia lab then prepared the piglet in cooperation with the anesthetist with a tracheal intubation and a bladder catheter. Also a vein was punctured for the administration of medication. When the preparation was done, the piglet was rotated to his left side, whereafter it was fixed again.

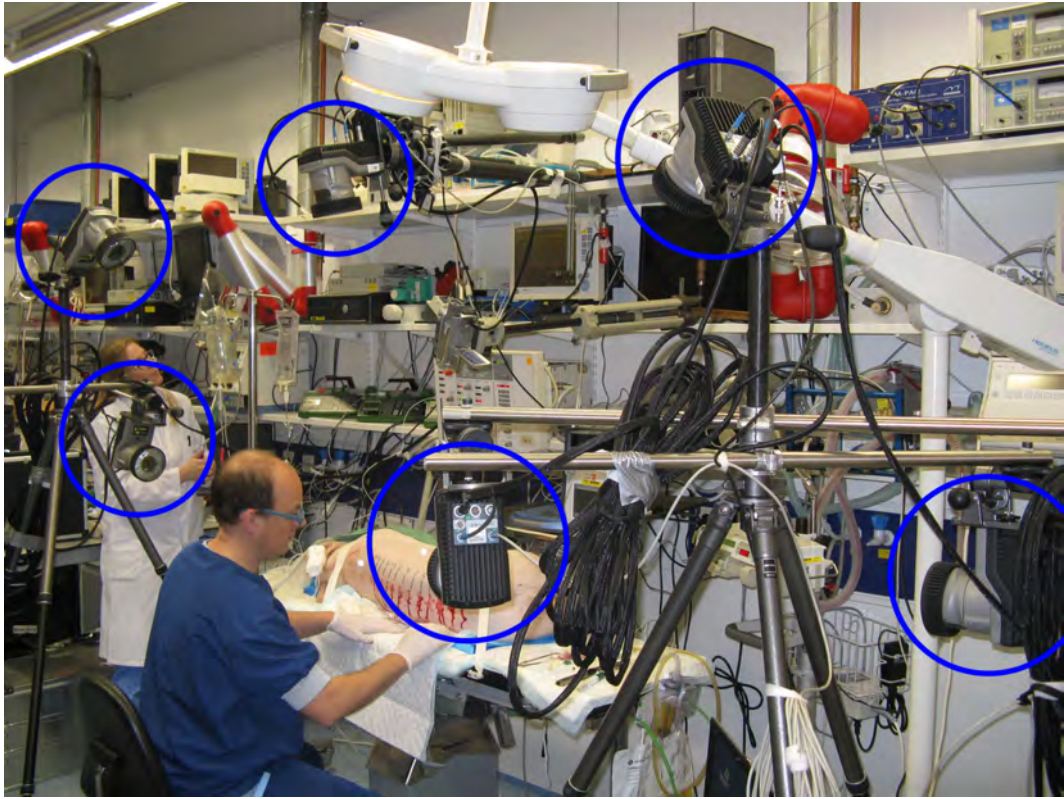
The table on which the piglet was fixed, was a specially made wooden plate which could be lifted, see figure B.9 and G.1, so the piglet could stay on the table during the CT-scan. In this manner, the tissue movement could be reduced to a minimum, so the CT-images could be used for extra data interpretation.

Three infrared markers of the Qualisys system were attached to the piglet before the CT-scan and stayed in place during the whole experiment, so the images of the CT could be linked to the position data.

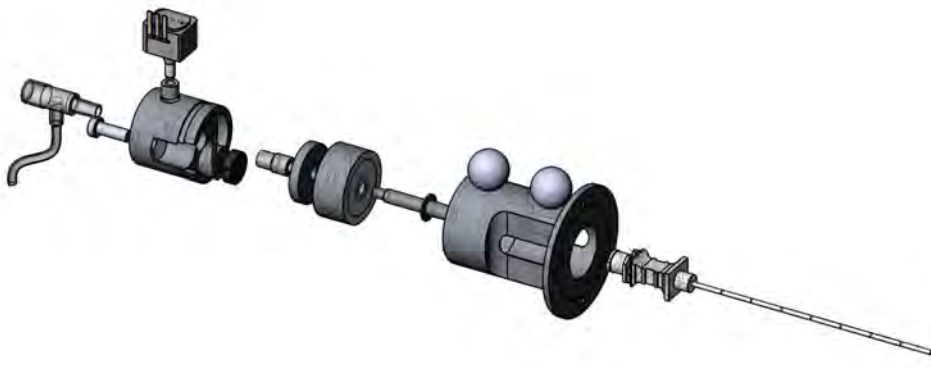
## B.5 Images



Figure B.1: *Overview research area*



**Figure B.2:** *Camera setup*



**Figure B.3:** *Exploded view measurement device*

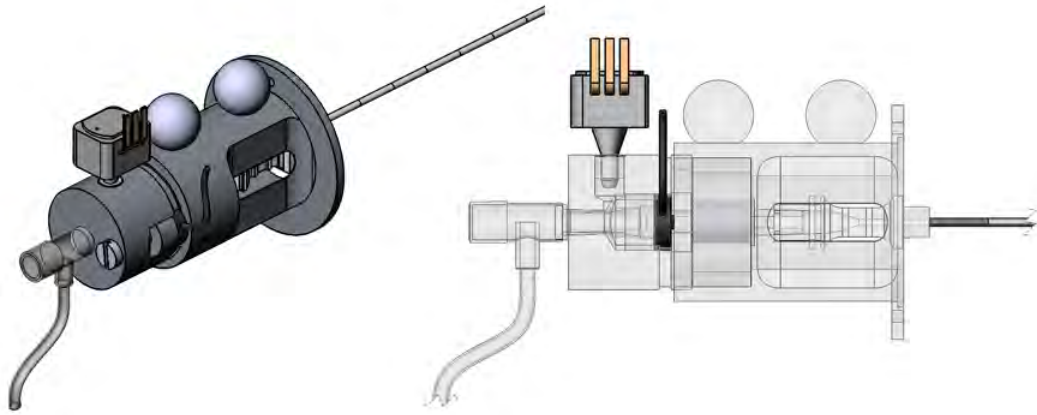


**Figure B.4:** *Measurement device, as can be seen the pressure-sensor is placed on top and the force-sensor is placed inside the device.*

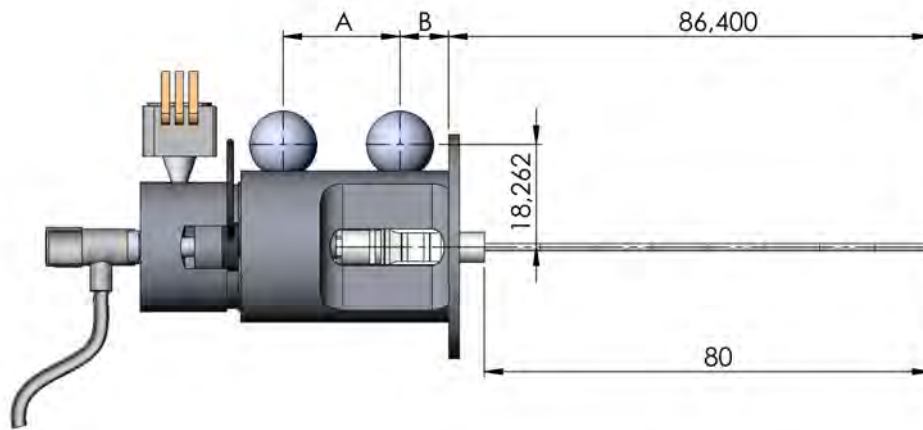


**Figure B.5:** *Important dimensions measuring device.*

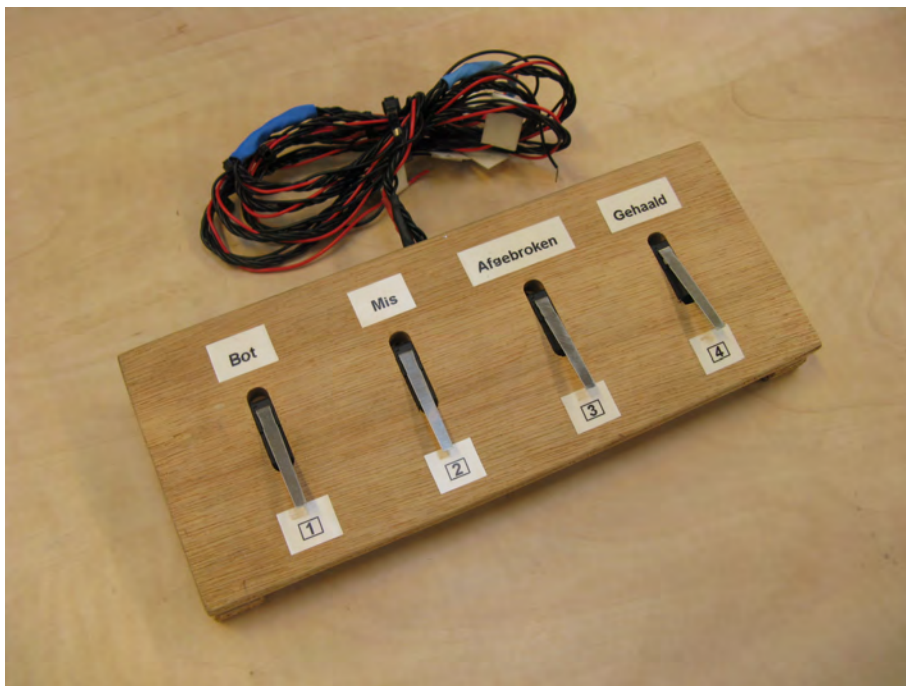


Figure B.6: *Additional input device*

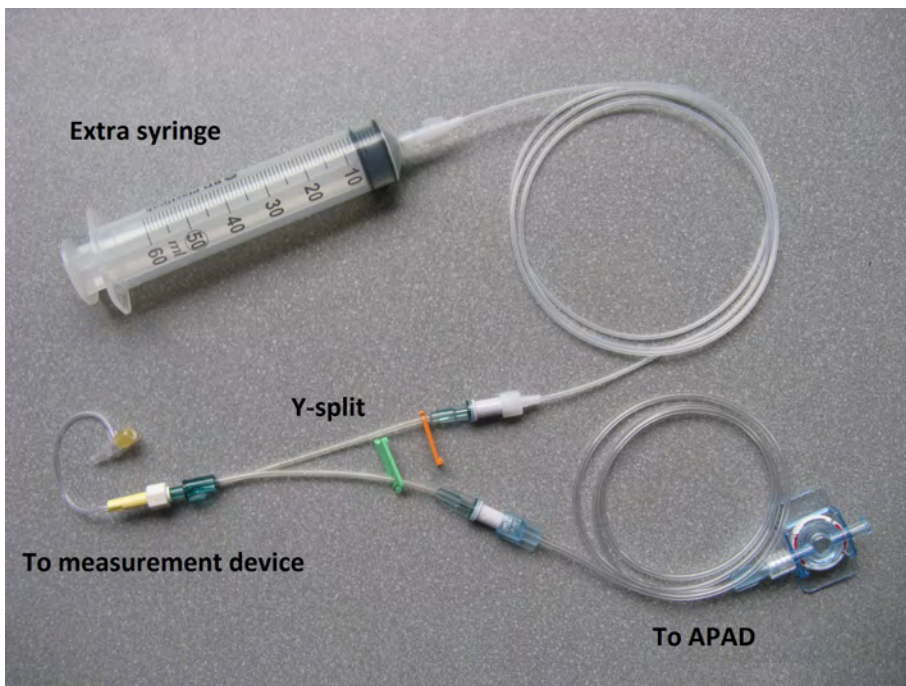


Figure B.7: *Extra syringe connected to the system with a Y-split.*



**Figure B.8:** *Preparation of the piglet.*





**Figure B.9:** *Transportation of the piglet*



**Figure B.10:** *CT-scan of the piglet*



**Figure B.11:** *Full prepared piglet with the three markers which also were in place during the CT-scan.*

## EXPERIMENT PROTOCOL

A protocol was written (in Dutch) in advance to capture the procedure. Both the anesthetist as the technician had to read this before the experiments started. This protocol is shown in the following paragraphs.

### C.1 Prepareren varken

Het varken wordt op de verrijdbare tafel gelegd. Het wordt vervolgens aan de tafel vastgebonden door middel van banden langs het schouderblad en banden langs het heupgewricht. De anesthesist identificeert de wervels d.m.v. tast en het echo apparaat en geeft de ruimte tussen de wervels streepsgewijs aan met een markeerstift, waarna deze tussenruimtes genummerd worden. De onderste wervel krijgt een 1, de wervel er boven een 2, etc. Naast de tussenruimtes worden ook de rand van de scapula en de os coxae duidelijk gemarkeerd. In de onderste wervel (S1) wordt een schroefje gedraaid. Op de CT-scan kan zo deze wervel worden gedentificeerd en als referentiepunt worden gebruikt. Met behulp van de CT-scan kunnen achteraf de overige wervels gedentificeerd worden. (De ruggenwervel formule van varkens is C7, T14-15, L6-7, S4, Cd20-23, wat in houdt dat zowel Thoracaal als Lumbaal, 1 wervel verschil tussen varkens aanwezig kan zijn.)

Nadat de wervels gedentificeerd zijn, wordt op alle insertie plaatsen, zowel mediaal als paramediaal aan beide zijden, de huid weg gestanst. Dit gebeurt met behulp van een 3mm diameter stans welke de huid tot 3mm diepte los stanst. De huid wordt vervolgens met behulp van een pincet en een mes verwijderd. Vervolgens wordt er een strook dubbelzijdige tape evenwijdig met de ruggenwervel, 1 cm boven de gestanste gaten geplakt. Op deze strook wordt de "Qualisys" marker boven de plek waar de eerste test plaats gaat vinden bevestigd. Na elke test wordt de marker van de strook verwijderd en op een nieuwe plaats op de tape bevestigd.

### C.2 Motion Capture

Voor de motion capture dienen minstens 6 camera's aanwezig te zijn. Deze camera's worden idealiter met een hoek van  $60^\circ$  (minimaal  $30^\circ$ ) van elkaar op de rug van het varken gericht. De zes camera's worden verdeeld over twee tripods die aan weerszijden van de tafel geplaatst worden. Door middel van extra statief-armen aan deze tripods kunnen de camera's boven het varken gepositioneerd worden. De kalibratie van de camera's wordt gedaan door de technicus. Tussen de wervels waar de naald ingebracht wordt, wordt een tracking ball d.m.v. een afgeknipte naald op/in de huid bevestigd. Nadat er wordt overgegaan op een volgende wervelhoogte, dient deze tracking ball verplaatst te worden.

## C.3 HD Camera

De HD camera dient boven het varken bevestigd te worden loodrecht op de beweging van de naald. Afhankelijk van de ruimte zal de camera tijdens de test eventueel verplaatst kunnen worden, zodat de inserties op verschillende hoogtes in de wervelkolom goed vastgelegd kunnen worden. De HD camera wordt aangesloten aan het motion capture systeem, zodat de metingen en opnames synchroon verlopen. Wanneer er zonder motion capture geprikt wordt, zal er een visuele aanwijzing moeten zijn dat de test is begonnen.

## C.4 Sensor Unit

Wanneer het motion capture systeem aanwezig is, wordt de sensorunit via de input unit van het motion capture systeem aangesloten. Als er zonder motion capture getest wordt, wordt de sensor unit via de LabJack UE9 aan de laptop aangesloten. Tijdens het prikken moet ten alle tijden voorkomen worden dat de naald aangeraakt wordt, aangezien dit direct invloed heeft op de meetresultaten.

## C.5 APAD

De disposable wordt met behulp van een met NaCl 0.9% gevulde 60 ml spuit ontlucht. De steriele APAD disposable wordt onder steriele omstandigheden gekoppeld aan een 60 ml spuit met Luer-Lock aansluiting en doorgespoeld met steriel NaCl 0,9%. Hierna wordt de spuit door de anesthesist in een infuus pomp geplaatst en wordt de druk-dome van de disposable op de APAD aangesloten. De infuus pomp wordt ingesteld op een inloopsnelheid van 100 ml/u en gestart en de APAD wordt aangezet. Wanneer men de knop START op de APAD activeert, moet er een duidelijke gelijkblijvende toon hoorbaar zijn en moet op het display de drukregistratie gaan lopen. Controleer de systeemdelen op lekkage en correcte aansluitingen. Terwijl de pomp loopt, wordt de opening van de slang door de anesthesioloog onder steriele omstandigheden enkele tellen geoccludeerd en weer losgelaten. Hierdoor zal de druk in het systeem oplopen en vervolgens terugvallen tot het uitgangspunt. Dit moet resulteren in een duidelijk hoorbare stijging in de toonhoogte en een oplopende curve op het display, en bij loslaten tot een plotse daling naar de beginwaarden. Na deze test kan de naald op de disposable worden aangesloten. Controleer op lekkage tussen naald en disposable. Wanneer er vloeistof uit de naaldpunt druppelt, kan er worden gestart met de punctie. Wanneer er geen stijging in toonhoogte hoorbaar is en/of de curve op het display niet oploopt, mag er niet gestart worden met de punctie. Dit geldt ook als bij loslaten de toon en/of de grafiek niet tot de beginwaarden terugvallen. De setup moet in dat geval gecontroleerd worden op correcte aansluitingen, lekkage, obstructie, defecten e.d. en na verhelpen van het probleem moet bovenstaande procedure opnieuw worden uitgevoerd. Na verificatie van de werking wordt de verkregen grafiek weggeschreven in een map. Hiermee wordt voorkomen dat deze waarden bij test data wordt opgeslagen.

De punctie kan ook niet worden gestart, wanneer er een alarmsignaal hoorbaar is (bijvoorbeeld: batterij alarm). Kijk op het display voor de oorzaak van het alarm en herstel de functie. Voer hierna de bovenstaande testprocedure uit. Mocht er om wat voor reden dan ook tijdens en punctie getwijfeld worden aan de werking van de APAD EL, bijvoorbeeld doordat de informatie die de anesthesioloog krijgt via zijn tastzin en verwachting niet overeenkomt met de audio-informatie, dan moet tijdens de punctie de werking van de APAD worden gecontroleerd. Zonder de naald verder op te voeren of terug te trekken, moet een occlusietest door de anesthesioloog worden uitgevoerd door het dichtknippen van de slang. Als blijkt dat de APAD en disposable normaal functioneren, kan de punctie worden vervolgd. Wel dient dit gemeld te worden en de technicus dient een event aan te maken in de metingen. Mocht de APAD en/of het disposable een defect vertonen, dan moet de punctie worden gestaakt.

1) Infuus pomp 2) Spuit, 50 ml 3) APAD 4) APAD disposable drukleiding 5) Sensorunit met epiduraal naald

## C.6 Draaiboek epiduraal punctie

Wanneer het varken geprepareerd is en de apparatuur genstalleerd, kunnen de testen beginnen.

	Anesthesist	Technicus
Stap 1	Prepareren varken volgens paragraaf 1.2	Opzetten Motion Capture systeem en HD camera volgens paragraaf 1.3 en 1.4
Stap 2	Varken naar CT-scanner	
Stap 3	Instellen APAD volgens paragraaf 1.6	Aansluiten sensorunit aan het Qualisys systeem.
Stap 4	APAD aansluiten op sensorunit.	Genereren van een random volgorde van insertieplaatsen d.m.v. Matlab script.
Stap 5	Wacht op het signaal van de technicus. Voer de epidurale naald hierna met een zo constant mogelijke snelheid en een zo constant mogelijk pad van de naald op in de richting van de epidurale ruimte. Concentreer u hierbij op "het gevoel aan de naald" en op het geluidssignaal dat u hoort. Wanneer de druk plots is gedaald: wacht enige seconden met de naald in positie terwijl de infuuspomp doorloopt op 100 ml/uur. Indien de druk stabiel laag blijft (tussen 2 en 8 kPa op het display), of slechts nog heel gering stijgt, weet u zeker dat de tip van de naald zich in de epidurale ruimte bevindt. De identificatie dient gemeld te worden aan de technicus. NB Een test kan niet worden gepauzeerd i.v.m. de opslagwijze van pauze-momenten op de APAD.	Startsignaal geven d.m.v. het woord "Start" en tegelijkertijd de schakelaar eenmalig kort indrukken. Apparatuur op werking controleren gedurende de test.
Stap 6	Na identificatie met de APAD wordt de sensor unit losgelaten. Naald niet terug trekken!	De data van de APAD wordt opgeslagen onder het nummer van de test (1, 2, 3, etc.) welke gedurende de dag hetzelfde blijft. Na identificatie van de epidurale ruimte dienen de meetgegevens opgeslagen te worden.
Stap 7	Met behulp van de echo probe wordt paramediaan een beeld gegenereerd van de ruggenwervel ter plaatse van de naald om een tweede identificatie te verkrijgen. Zo mogelijk wordt dit beeld opgeslagen. Aangezien boven de insertieplaats het Qualisys bolletje bevestigd is, wordt de echo probe aan de onderzijde van de ruggengraad geplaatst.	Wanneer er geen dubbele identificatie plaats vindt, dient dit duidelijk op het meet formulier aangegeven te worden.
Stap 8	Na de tweede identificatie kan de naald worden teruggetrokken, waarna een volgende insertie plaats aan de beurt is.	De volgorde van insertieplaatsen wordt bepaald door Matlabscript die de volgorde randomiseert.

## C.7 Het prikken

De volgorde van de te prikken tussenruimtes wordt meegedeeld door de technicus. Per tussenruimte wordt er eerst mediaal, vervolgens paramediaal (boven, d.w.z. rechterzijde) en tenslotte paramediaal (onder, d.w.z. linkerzijde) Naast de standaard testen met de APAD, ook n of meerdere keren:

- Naald met de tip in epidurale ruimte tijdens de CT-scan

Alle gebruikte epiduraal naalden dienen bewaard en gelabeld te worden, zodat ze later microscopisch bekeken kunnen worden op slijtage.

## C.8 Invulformulieren

During the tests all values of the experiment were written on an entry form, see figure C.1, in order to handle all data of the motion capture system.

**Meetformulier testen (met Qualisys systeem)**  
Epiduraal prikken op varkens

Test: Nr. \_\_\_\_\_

Datum: \_\_\_\_\_

Aansprekend: \_\_\_\_\_

Tijdstip aanvang test: \_\_\_\_\_

Tijdstip einde test: \_\_\_\_\_

**Varken**

Gewichtsklasse	30 kg
Sexe	Manneijk
Totaal aantal wervels (n) (incl. cervicale hyperflexie)	12 stuks
Hoofdwervel wervels Lumbaal	
Hoofdwervel wervels Thoracaal	

**Naald**

Dikte	18 Gauge
Langte	8 cm
Bevel	Tip to cranial direction

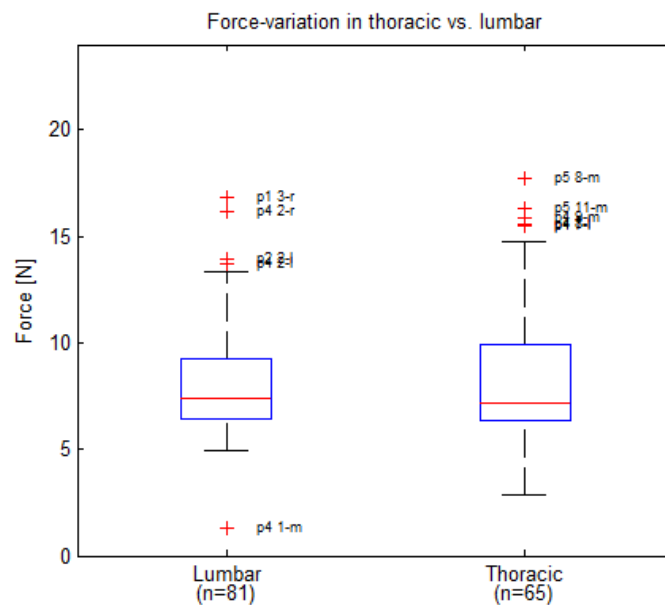
Nummer test	Wervelruimte (N, T1-12, L1-5, Th1-12)	Naam APAD (Bevel)	Diepte insertie (in cm)	Operatoren (P, B, A, M, A, S, D)	Extra opmerkingen
1				P, B, A, M, A, S, D	
2				P, B, A, M, A, S, D	
3				P, B, A, M, A, S, D	
4				P, B, A, M, A, S, D	
5				P, B, A, M, A, S, D	
6				P, B, A, M, A, S, D	
7				P, B, A, M, A, S, D	
8				P, B, A, M, A, S, D	
9				P, B, A, M, A, S, D	

Figure C.1: Entry form for during the test

## RESULTS

This chapter presents an overview of the main results of the experiments. The results are presented for the force measurements, distances between force- and pressure event, force-position data and pressure measurements. All presented results contain the measurement data of the five piglets, except those concerning pressure, where the second experiment is excluded due to a disfunctional pressure sensor. All results are showed with their sample size.

Due to the manual insertion of the needle, it was hard to obtain an accurate force-position relationship. The position data is noisy and due to the alternating inward and outward movements it is difficult to interpret. The position data was filtered by a 2nd order low pass Butterworth filter with a cutoff frequency of 30Hz, since people can only generate position data up to 25 Hz. This filtered data was plotted against the force-data.



**Figure D.1:** Force variation between lumbar region (L5-L6 until Th15-L1) and the thoracic region (Th14-Th15 until Th9-Th10)



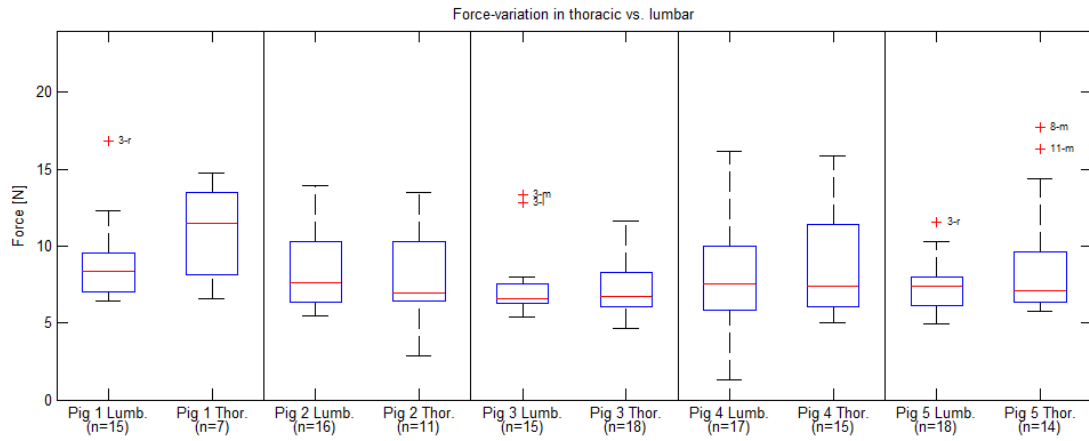


**Figure D.2:** Force variation between lumbar region (L5-L6 until Th15-L1) and the thoracic region (Th14-Th15 until Th9-Th10), shown per pig

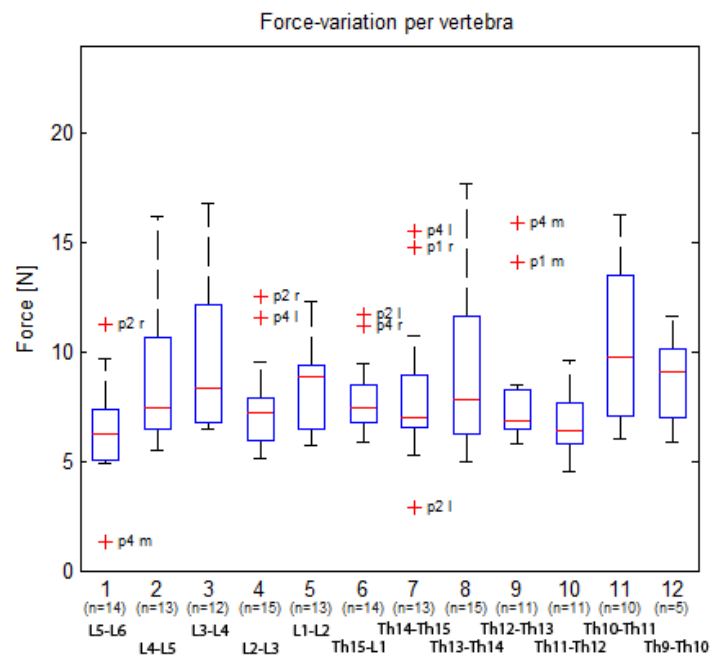


**Figure D.3:** Force variation between the different vertebrae.

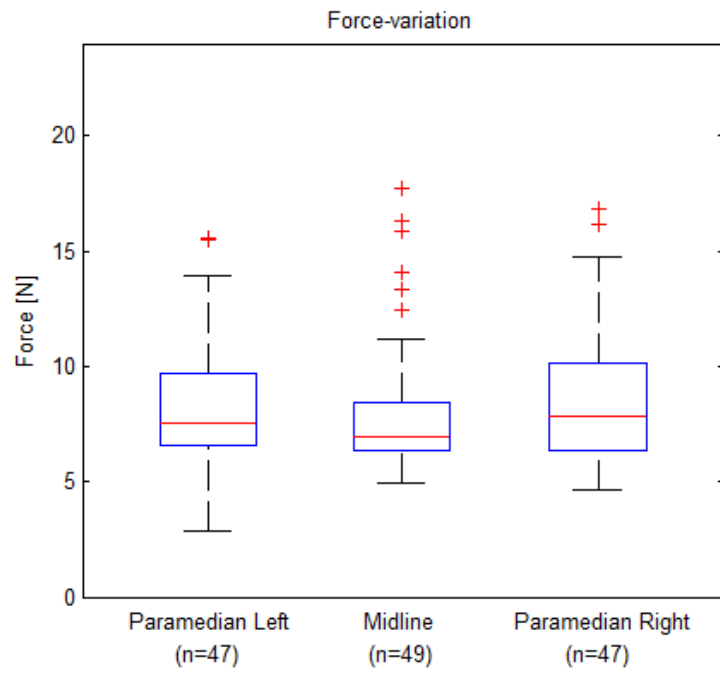


Figure D.4: Force variation between the different ways of approaching the epidural space.

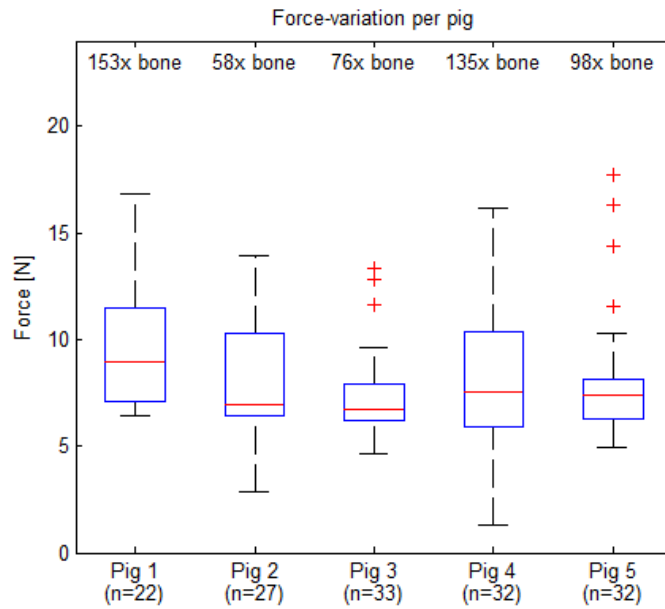
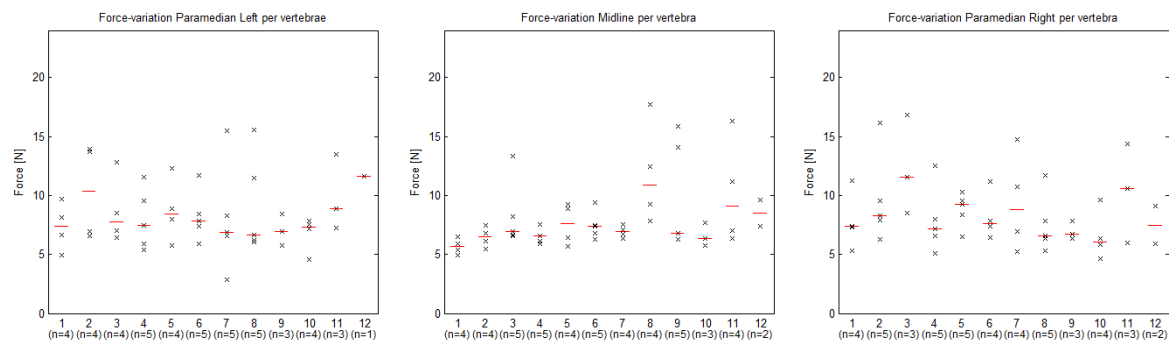
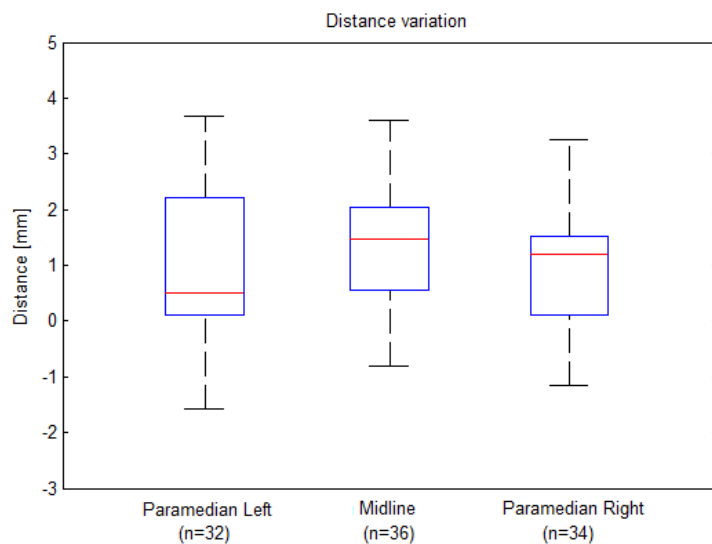


Figure D.5: Force variation between the different piglets.



**Figure D.6:** Force variation between the different ways of approaching the epidural space shown per vertebra.



**Figure D.7:** Variation in distance between the pressure-drop and the force-drop. A positive value indicates the occurrence of the force-peak before the pressure-drop.

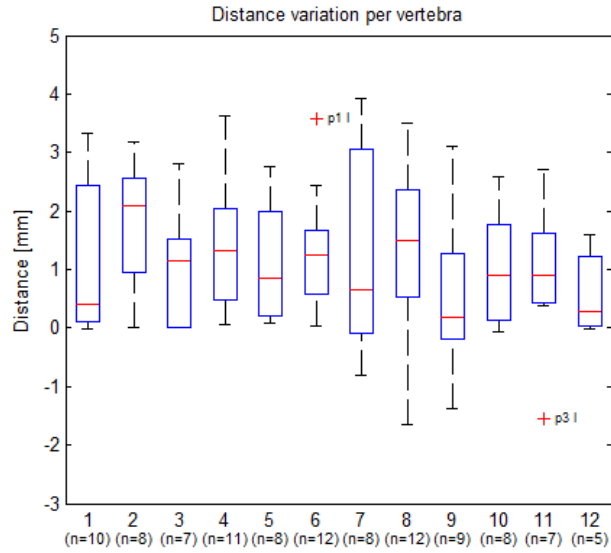


**Figure D.8:** Variation in distance between the pressure-drop and the force-drop observed between the vertebrae. A positive value indicates the occurrence of the force-peak before the pressure-drop.

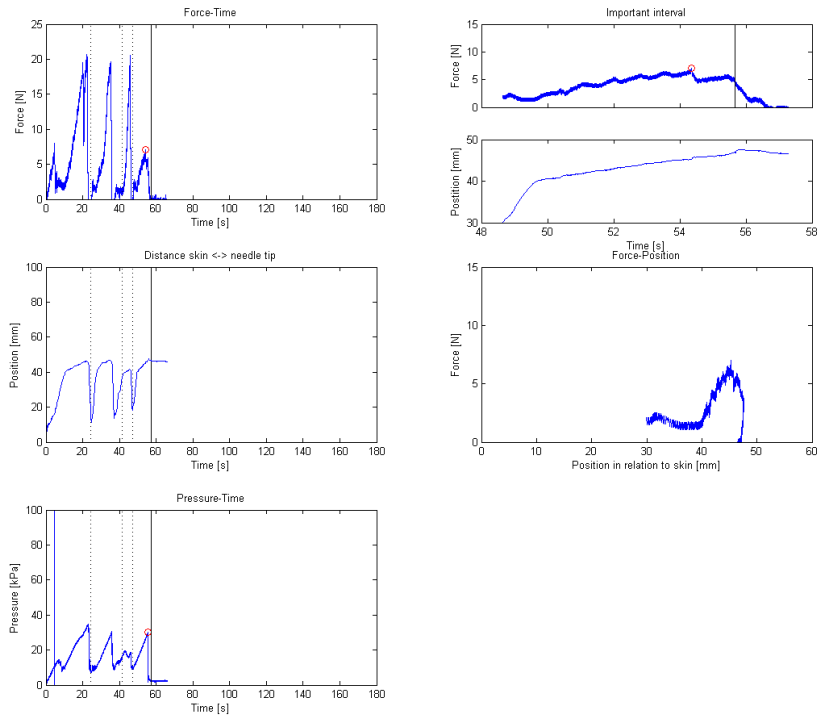


**Figure D.9:** Example 1; Upper left: Force-time, Mid left: Displacement-time, Bottom left: Pressure-time, Upper right: Important interval of Force- and pressure-time, Mid-right: Force-position graph

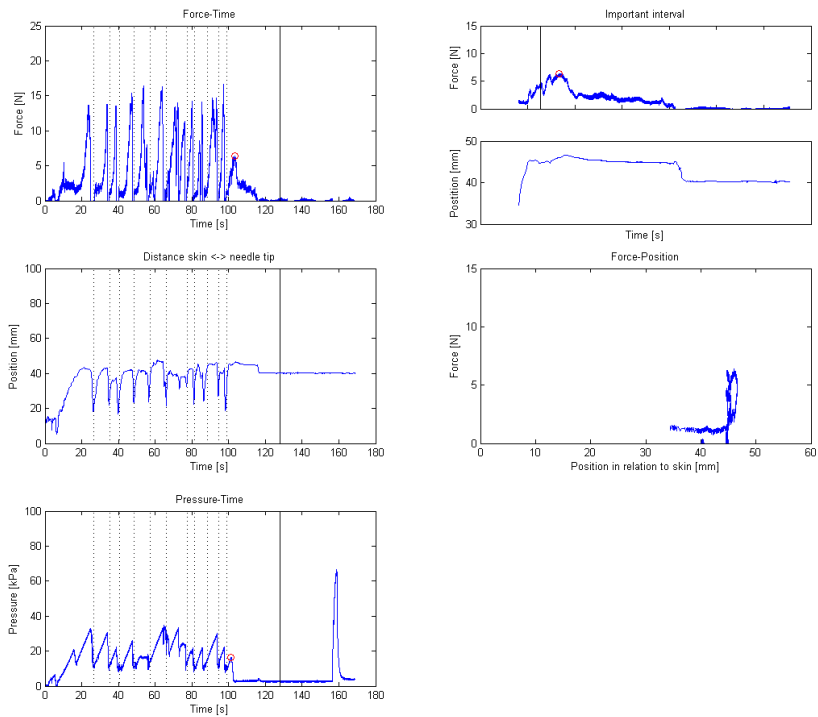


**Figure D.10:** Example 2; Upper left: Force-time, Mid left: Displacement-time, Bottom left: Pressure-time, Upper right: Important interval of Force- and pressure-time, Mid-right: Force-position graph

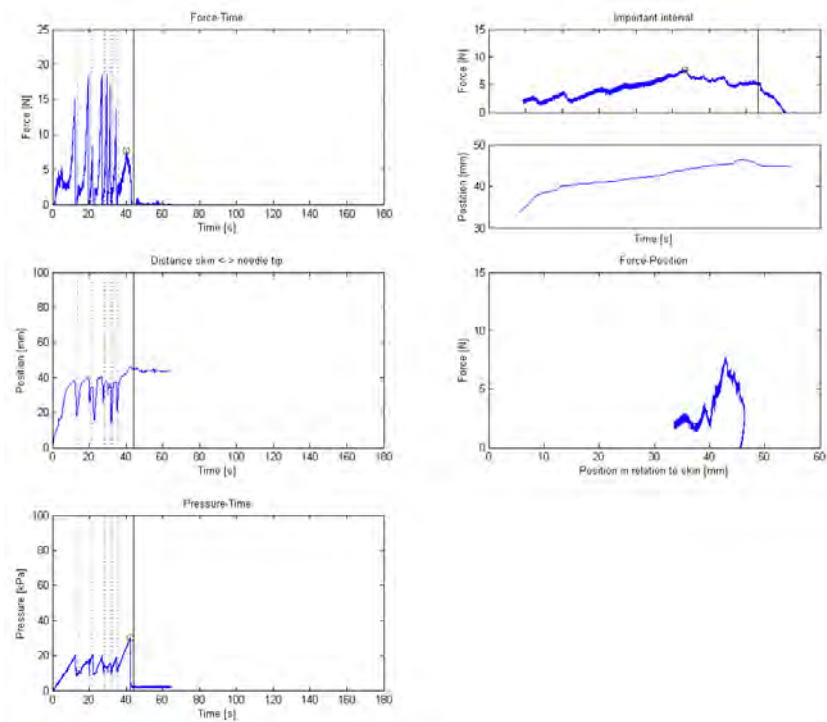


**Figure D.11:** Example 3; Upper left: Force-time, Mid left: Displacement-time, Bottom left: Pressure-time, Upper right: Important interval of Force- and pressure-time, Mid-right: Force-position graph

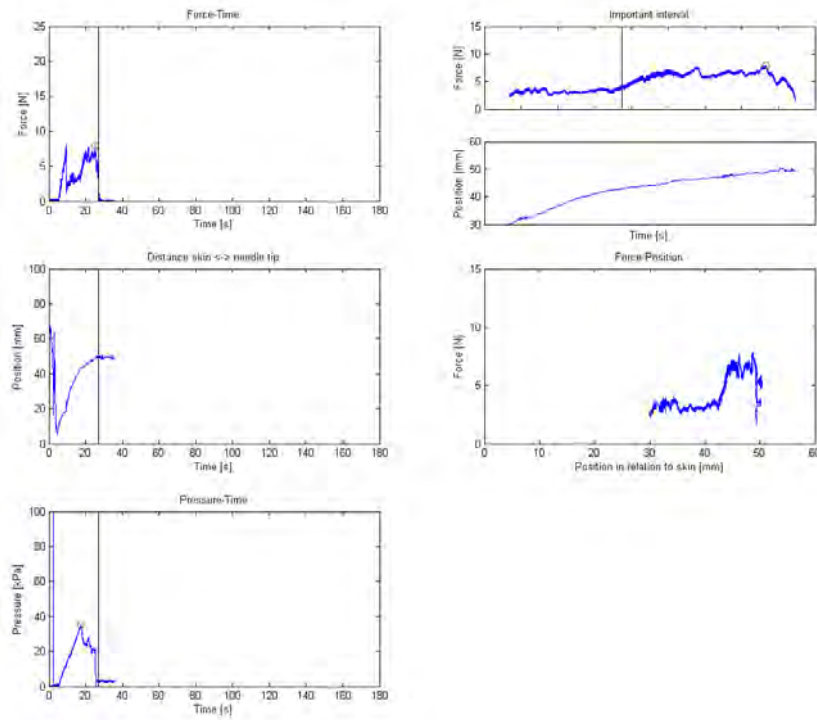


**Figure D.12:** Example 4; Upper left: Force-time, Mid left: Displacement-time, Bottom left: Pressure-time, Upper right: Important interval of Force- and pressure-time, Mid-right: Force-position graph

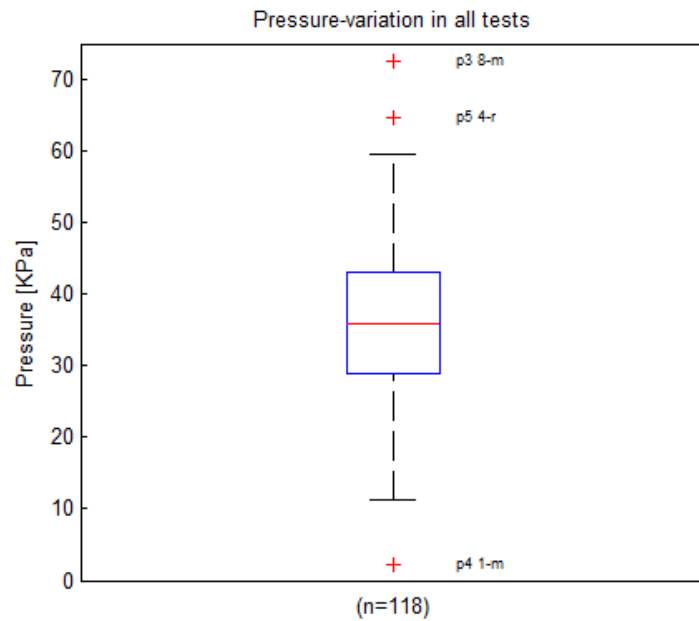


**Figure D.13:** Height of the pressure-peaks. The red line is the median, the edges of the box are the 25th and 75th percentiles and the whiskers extend to the most extreme datapoint within 1.5 times interquartile range of resp. the first and third quartile.

## STATISTICS

In order to make the measurement results of the force-data manageable for the the epidural simulator they will have to be reduced to a normal distribution. The data consist of only positive values, with also a high risk of data points above average, as measured forces will be lower rather than higher, for example by puncturing stiffer tissue than average. Therefor the data had to be transformed to gain an normal distribution. Normally these transformations are used to compare different data sets with the use of statistical analysis methods, but since the force-peak data are used for input of the simulator, only the transformation in applied. By back transforming the mean, the geometric mean can be obtained.

The transformations were done with the use of SPSS.

## **E.1 Transformations**

To transform positive skewed data to a normal distribution there are some standard mathematical tricks available. These different mathematical transformations were compared, form which the histograms and the normal distribution are showed.

### **E.1.1 Without transformation**

The untransformed data is obviously positive skewed, see figure E.1.

### **E.1.2 Natural logarithmic transformation**

The natural logarithmic transformation delivers clear improvement, see figure E.2, although the histogram has a much higher peak then the normal distribution of the data.

### **E.1.3 Common logarithmic transformation**

To improve the natural logarithmic transformation, a log to base 10 was tried. This improved the difference between the peak of histogram and the normal distribution of the data, see figure E.3. Also other base numbers where checked, but this did not change the skewness or kurtosis of the transformed data and therefore not further investigated.

### **E.1.4 Square root transformation**

To verify the other mathematical transformation methods, also a square root transformation was applied. As can be seen in figure E.4 this does not provide any improvement.

### **E.1.5 Square transformation**

Also a square transformation was tried, but as can be seen in figure E.5, it only got worse.

### **E.1.6 Twice the common logarithmic transformation**

In order to improve the logarithmic transformation, also a logarithmic transformation of the transformation was done, see figure E.6. Although this visually looks better, the skewness and kurtosis are not improved. Also the obtained mean is difficult to interpret and therefore this transformation was rejected.

### **E.1.7 Reciprocal transformation**

As last transformation also an reciprocal transformation was done, see figure E.7. As can be seen, this does not fit better than the logarithmic transformation. Also the left tail of the normal distribution goes negative, which is not possible with the peak-forces. Therefore this transformation was rejected.

### **E.1.8 Descriptive statistics**

After the visual comparison of the different transformation techniques, also a statistic comparison was done. The kurtosis and the skewness of the different transformation was calculated and compared. A skewness of 0 means that the data is normal distributed. Positive values of kurtosis indicate a pointy distribution, whereas negative values indicate a flat distribution. For a good fit a skewness and kurtosis close to zero are desirable.

As can be seen in the following table, figure E.8, the skewness and kurtosis of both logarithmic transformations and the square transformation are the best fit to a normal distribution. Together with the visual fit of the normal distribution and the difficulty of interpreting the square transformed data, the choice was made for the logarithmic to base 10 transformation. The lognormal distribution is often used for transforming data which have positive skewness to a normal distribution. By back transforming the mean of the log10 transformation by taking the antilog, the so called geometric mean can be estimated. The geometric mean is less than the mean of the raw data. A major difference with the normal distribution is the multiplicative standard deviation  $s^{(*)}$  instead of an additive standard deviation  $s$ . This means that to calculate the 68.3% interval of confidence, the mean times or divided by the multiplicative standard deviation gives the correct values. The  $x/$  sign corresponds to the established sign  $\pm$ .



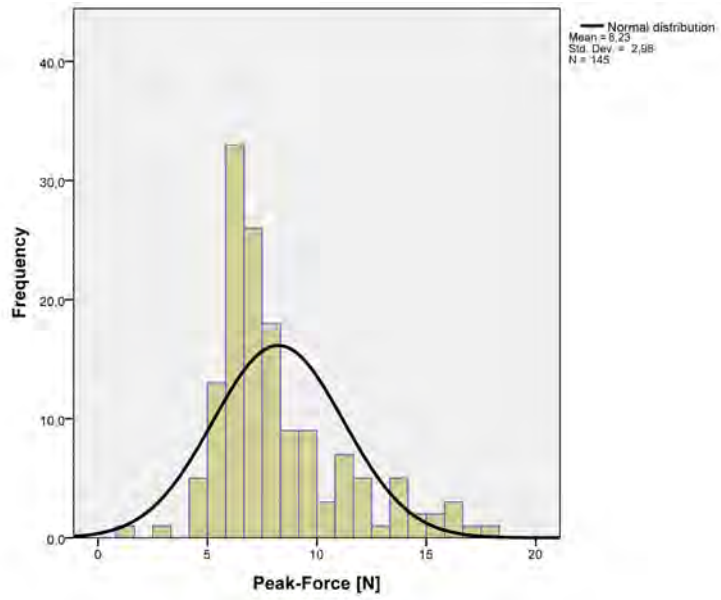


Figure E.1: Force peaks; skewed normal distribution

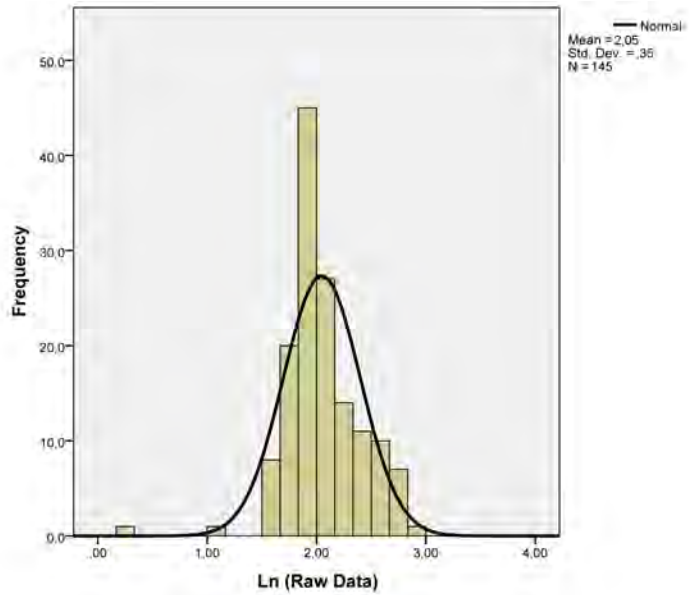


Figure E.2: Force peaks; Ln transformed distribution

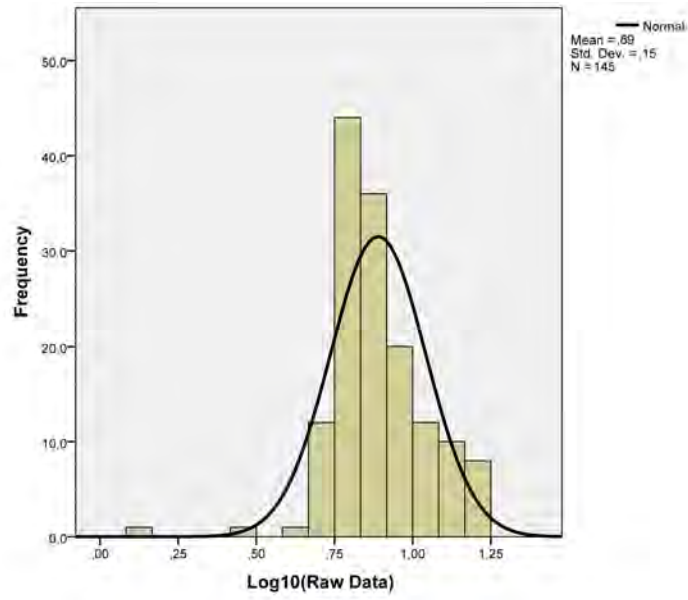


Figure E.3: Force peaks; Log10 transformed distribution

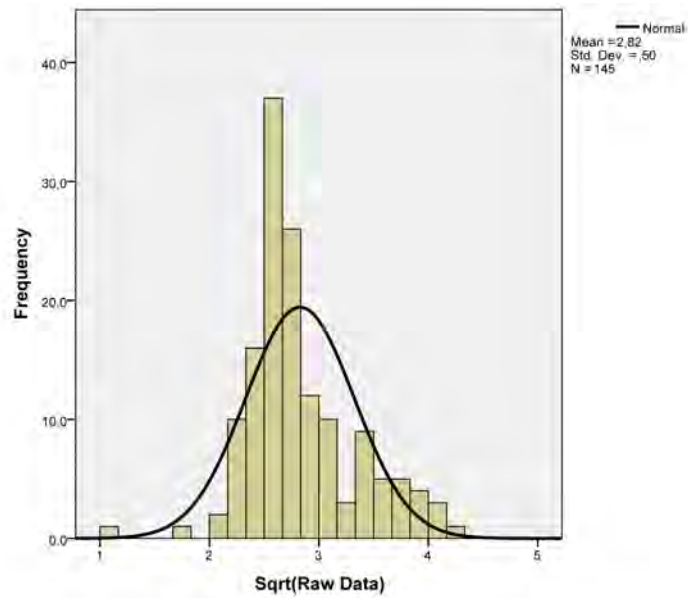


Figure E.4: Force peaks; Sqrt transformed distribution

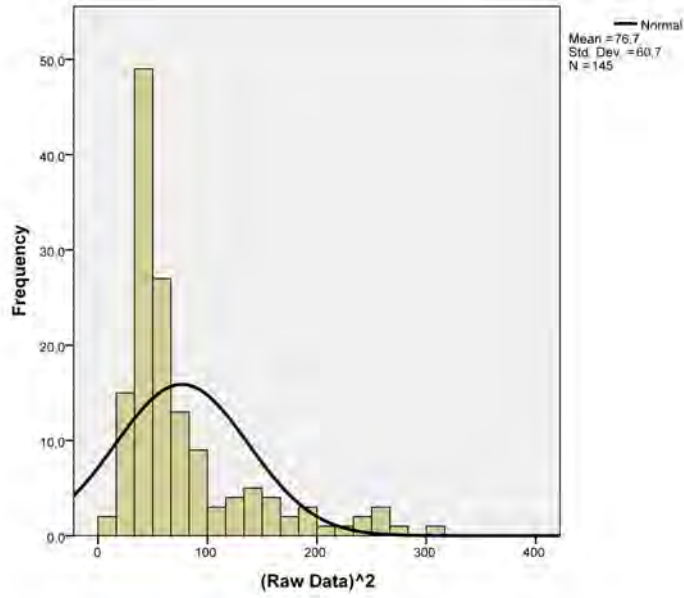


Figure E.5: Force peaks; Squared transformed distribution

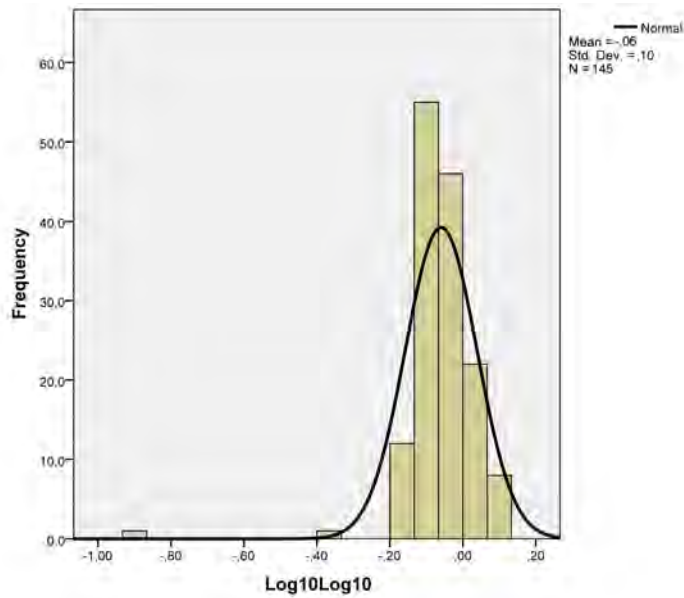


Figure E.6: Force peaks; Log10(Log10) transformed distribution

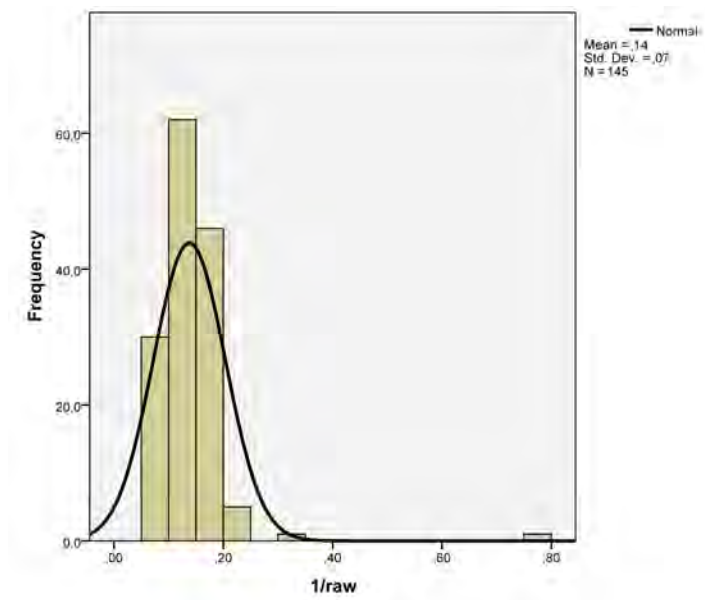


Figure E.7: Force peaks; Reciprocal transformed distribution

Descriptive Statistics

	N	Mean	Std. Deviation	Skewness		Kurtosis	
	Statistic	Statistic	Statistic	Statistic	Std. Error	Statistic	Std. Error
Raw	145	8,2374556007	2,9847343973	1,187	,201	1,144	,400
Ln	145	2,0482	,35257	-,408	,201	3,883	,400
Log10	145	,8895	,15312	-,408	,201	3,883	,400
Sqrt	145	2,8272	,49623	,632	,201	,978	,400
Squared	145	76,4265	60,95272	1,870	,201	3,160	,400
Log10Log10	145	-,0594	,09832	-4,657	,201	40,369	,400
devidedbyraw	145	,1380	,06598	5,961	,201	54,419	,400
Valid N (listwise)	145						

Figure E.8: Descriptive statistics

## DATA ANALYSIS

## F.1 Qualisys

In an ideal situation the Qualisys motion capture system recorded on path per marker. Since the experiment location was far from ideal, with fluorescent lighting and little room for the cameras this resulted in much distraction in the capture.

The enclosed Qualisys program, see figure F.4, ensured that when a marker was out of range of the cameras for more than 10 frames, a new path was created. This resulted, with a sample rate of 200hz, in many different paths that had to be manually linked together.

The output of the Qualisys Motion Capture system consisted of the X-,Y- and Z-coordinates of the 6 markers, which could be loaded in Matlab.

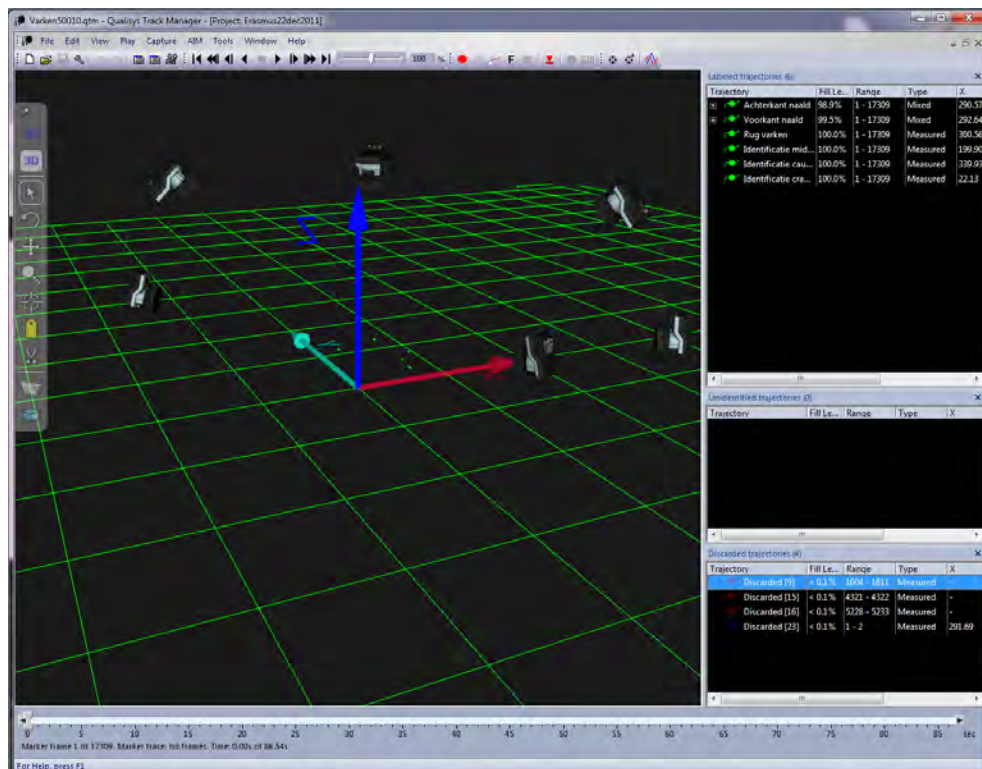


Figure F.1: Snapshot from Qualisys Track Manager

## F.2 Matlab

To analyse the in total 180 data sets with position, force and pressure data a Matlab scrip was written. In this script the bone-contacts and wrong insertions were collected. If during the measurements more then 7 times bone-contact occurred or if for any other reason the measurement was aborted, the force results were ignored. Also if the anesthetist suspected that he had reached the epidural space via bone, the test results were excluded.

In Matlab an interface was made to ensure the functionality of the peak selection. In this interface, see figure F.2, a specific piglet and test could be selected, after which the force-time, position-time, pressure-time and the by the algorithm selected interval of only inward movement of the needle of the force-time and position-time graphs were shown. In these graphs the force-peaks and pressure-peaks selected by the algorithm were indicated and could be visually inspected. An examples of the collected data is given in figureF.2.

To obtain the displacement of the needle, the unitvector of the two markers on the needle were determined. With the known dimensions of the measurement device and the needle the place of the needle tip could be calculated, see figure F.4.

A marker which was placed 10 mm above the paramedian right insertion place was used to calculate the insertion places. This marker was replaced when another level was punctured. In the matlab script the z-coordinate of this marker was corrected with 10, 20 or 30 mm for respectively the paramedian right, midline and paramedian left approach. It was assumed that the back of the pig is flat and lay perpendicular to the table.

```
1 %% Length between markers on sensor-unit
2 needle.x = points(2).x-points(1).x;
3 needle.y = points(2).y-points(1).y;
4 needle.z = points(2).z-points(1).z;
5 dist_needlemarkers = sqrt(((needle.x).^2+(needle.y).^2)+needle.z.^2);
6
7 % Unitvector of the needle
8 needle.ex = needle.x./dist_needlemarkers;
9 needle.ey = needle.y./dist_needlemarkers;
10 needle.ez = needle.z./dist_needlemarkers;
11 needle.ev = sqrt(((needle.ex).^2+(needle.ey).^2)+(needle.ez).^2);
12
13 % Determining position of the needle tip
14 m_n_dist = 18.262; % marker to needle ...
15 distance (see SolidWorks Drawing)
16 omega = acos(sqrt((needle.ex).^2+(needle.ey).^2)./needle.ev);
17 beta = atan(needle.ex./needle.ey);
18 n_extra = m_n_dist*sin(omega);
19 needle.startx = points(2).x+(n_extra.*sin(beta));
20 needle.starty = points(2).y+(n_extra.*cos(beta));
21 needle.startz = points(2).z-(m_n_dist*cos(omega));
22 var = [0.75+0.6 1.2+0.6 2.71+0.6 1.9+0.6 2.68+0.6]; % Variation in ...
23 distances front marker between experiments
24 needle.tipx = needle.startx+(needle.ex.*(80.2+6.2+var(s))); % Coordinates of the ...
25 needle.tipy = needle.starty+(needle.ey.*(80.2+6.2+var(s))); % Coordinates of the ...
26 needle.tipz = needle.startz+(needle.ez.*(80.2+6.2+var(s))); % Coordinates of the ...
27 tip of the needle (see SolidWorks Drawing)
28 needle.tipz = needle.startz+(needle.ez.*(80.2+6.2+var(s))); % Coordinates of the ...
29 tip of the needle (see SolidWorks Drawing)
30
31 % Displacement back of the pig <-> needle tip
32 needle.disp = sqrt(((needle.tipx-points(3).x).^2+(needle.tipy-(points(3).y)).^2)...
33 ...+(needle.tipz-(points(3).z)).^2);
```

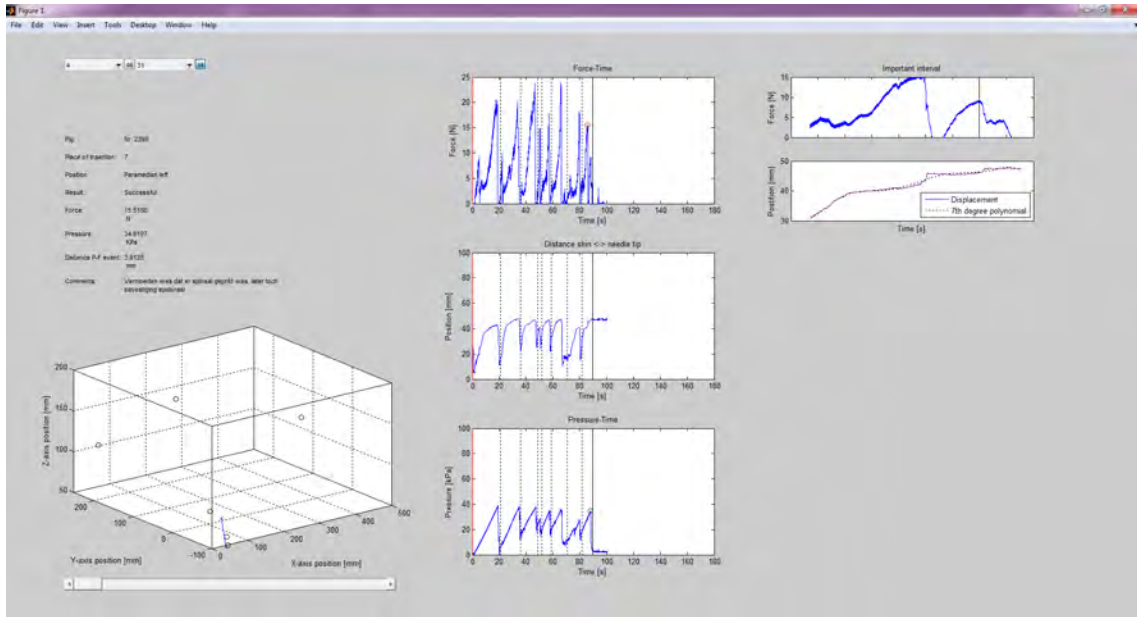


Figure F.2: Screenshot Matlab-analysis.

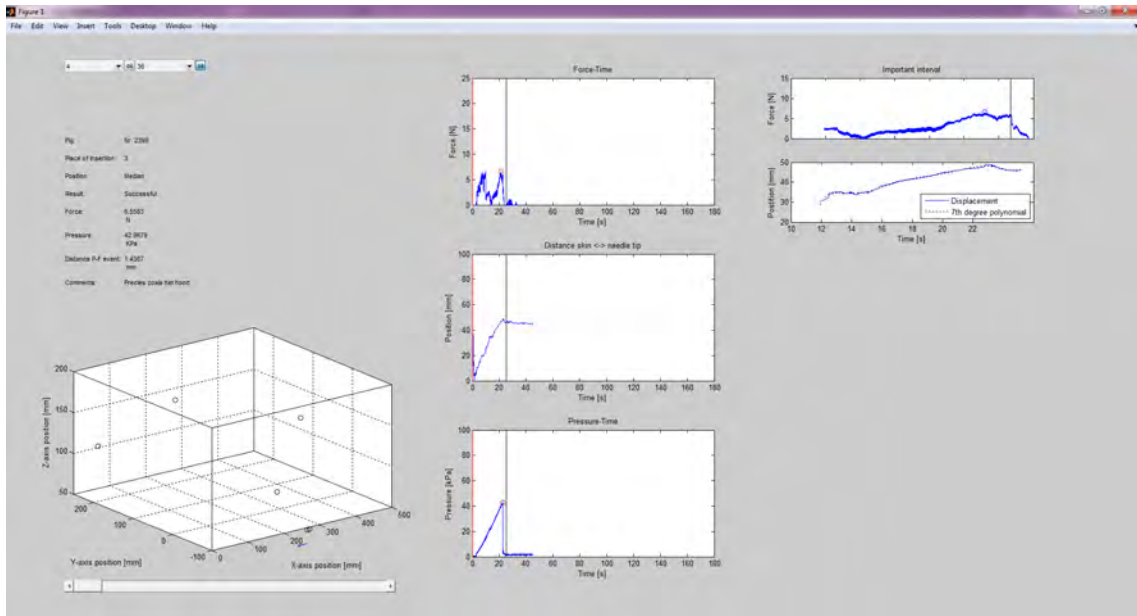
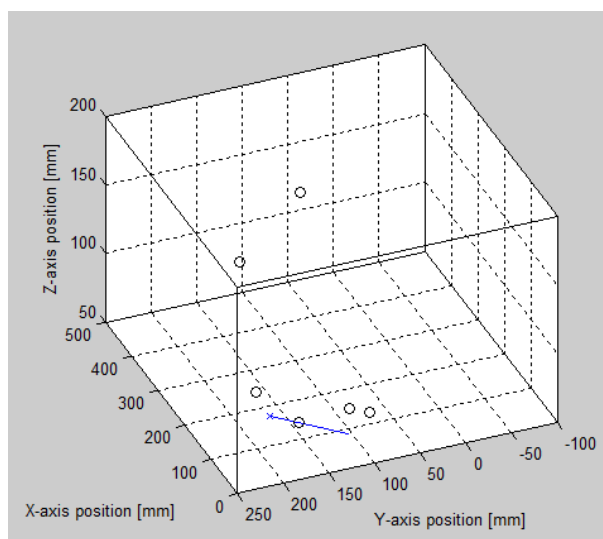


Figure F.3: Screenshot 2 Matlab-analysis.



**Figure F.4:** Snapshot from the calculated needle in Matlab. The 3D representation was used for visual inspection of the needle displacement.



## CT-SCAN

For additional understanding of the anatomy of the pig, five piglets were scanned using an CT-scanner. The first piglet was a pilot test and the other four were scanned before the experiments



**Figure G.1:** *Vertebral column of a piglet (CT-scan of pilot 5)*

took place. Piglet 1 of the experiments was not scanned.

In this way, the vertebral column could be studied. In fig.G.2 it can be seen that the intervertebral opening between Thoracic 8 and Thoracic 9 is so small that the chance of reaching the epidural space is very small. Therefore was decided that the experiment setup would start from the intervertebral opening Thoracic 9-Thoracic 10. During the experiments it appeared that this one is also very difficult to achieve, although it has been achieved a number of times. In fig.G.3 it can be seen that the opening is much larger and therefore the chance of bone-contact is less.

For extra perception, also a scan with a needle tip inside the epidural space was made. Just before the scan the anesthetist applied the loss-of-resistance technique in order to confirm right placement.

The program which was used to interpret the CT images, OsiriX - Dicom viewer, simulated the metal parts as bone parts. The scattering due to the metal creates a somewhat thicker representation of the needle than is the case in reality. There must be to be mentioned that the settings of the CT scanner were focused on bone tissue, which causes the bones are displayed slightly larger than they are in reality. The intermediate spaces in the figures G.2 and G.3, are in fact slightly larger.

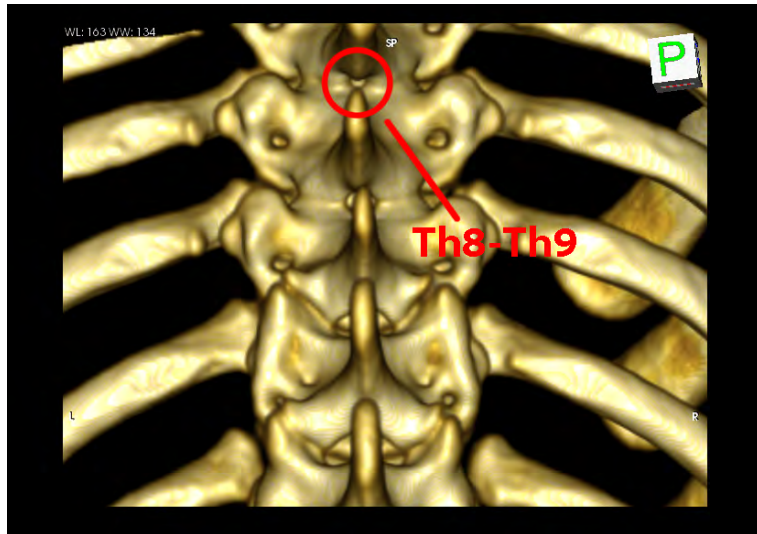


**Figure G.2:** *Passage between vertebrae Th8-Th9 (CT-scan of pilot 5)*

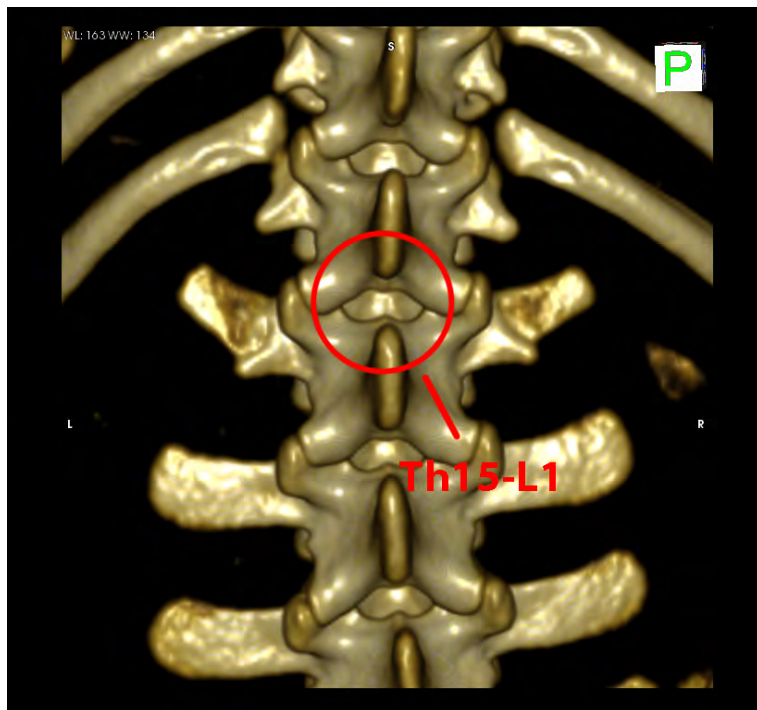


**Figure G.3:** *Passage between vertebrae Th15-L1 (CT-scan of pilot 5)*



**Figure G.4:** *Epidural needle applied between L4-L5*